1/25

# RADIONUCLIDE SORPTION IN THE ALLUVIUM AT YUCCA MOUNTAIN, NEVADA—A PRELIMINARY DEMONSTRATION OF AN APPROACH FOR PERFORMANCE ASSESSMENT

*Prepared for*

**Nuclear Regulatory Commission**
**Contract NRC-02-97-009**

*Prepared by*

**David R. Turner**
**Gordon W. Wittmeyer**
**F. Paul Bertetti**

**Center for Nuclear Waste Regulatory Analyses**
**San Antonio, Texas**

**June 1998**

# ABSTRACT

One of the Key Technical Issues identified by the Nuclear Regulatory Commission is focused on processes that control potential radionuclide transport from the proposed high-level radioactive waste repository at Yucca Mountain, Nevada (YM), through the natural barriers of the geological setting. One of these processes is the sorption of radionuclides onto minerals in the alluvium. Radionuclide sorption, expressed in terms of sorption coefficients ($K_D$), is controlled by water chemistry and by the mineralogy and mineral surface area exposed in fractures and matrix pores. In this report, an initial approach is outlined that will allow incorporation of more detailed models that take into account the geochemical dependence of radionuclide sorption into performance assessment (PA). Geochemical speciation models are used to evaluate the effects of different geochemical parameters on sorption and to calculate response surfaces that reflect radionuclide sorption as a function of key geochemical parameters.

To obtain a mechanistic basis for sorption behavior for PA, a diffuse-layer surface complexation model is applied to calculate Np(V) sorption on montmorillonite for a wide range in geochemical parameters such as M/V, pH, $PCO_2$, and radionuclide concentration. Neptunium sorption, normalized to effective mineral surface area ($K_{A'}$), is influenced most by pH and $PCO_2$. Because Np(V) sorption behavior as a function of geochemistry is similar for different types of aluminosilicates, the effective mineral surface area can then be used as a scaling factor to convert $K_{A'}$ to $K_D$ for use in PA transport calculations. A response surface for Np(V) sorption as a function of pH and $PCO_2$ is developed, and possible ways of incorporating the results into PA are investigated.

# ACKNOWLEDGMENTS

This report was prepared to document work performed by the Center for Nuclear Waste Regulatory Analyses (CNWRA) for the Nuclear Regulatory Commission (NRC) under Contract No. NRC-02-97-009. The activities reported here were performed on behalf of the NRC Office of Nuclear Material Safety and Safeguards (NMSS), Division of Waste Management. The report is an independent product of the CNWRA and does not necessarily reflect the view or regulatory position of the NRC.

# QUALITY OF DATA, ANALYSES, AND CODE DEVELOPMENT

**DATA:** CNWRA-generated original data contained in this report meet quality assurance requirements described in the CNWRA Qaulity Assurance Manual. Sources for other data should be consulted for determining the level of quality for those data.

**ANALYSES AND CODES:** The MINTEQA2, Version 3.11 computer code was used for analyses contained in this report. This computer code is controlled under CNWRA Software Configuration Procedures. The spreadsheet software Microsoft Excel 97 was used in calculations, and the curve-fitting software TableCurve 2D and TableCurve 3D from Jandel Scientific were used to fit data presented here. These are commercial software packages and only the object codes are available to the CNWRA.

# CONTENTS

# FIGURES

# FIGURES (cont'd)

6/25

# TABLES

# 1 INTRODUCTION AND REGULATORY BACKGROUND

One of the primary objectives of the Nuclear Regulatory Commission (NRC) refocused prelicensing program is to direct activities toward resolving the 10 key technical issues (KTIs) it considers most important to performance of the proposed high-level nuclear waste (HLW) repository at Yucca Mountain, Nevada (YM). One of these KTIs is concerned with assessing the potential for radionuclide transport (RT) from the repository through the subsurface to the accessible environment.

In the July 1996 U.S. Department of Energy (DOE) Waste Containment and Isolation Strategy (WCIS) (U.S. Department of Energy, 1996) and the January 1998 Repository Safety Strategy (RSS) (U.S. Department of Energy, 1998), reduction in radionuclide concentrations by geochemical processes during RT is mentioned as a key hypothesis that needs to be tested in any site suitability demonstration for a proposed repository at YM. Specifically, chemical properties of the system barriers (natural and engineered) that reduce concentrations during RT (RSS–Hypothesis 14) need to be examined and evaluated. The likely mechanism to address this issue involves quantitative conceptual and numerical models in repository performance assessment (PA) describing RT under geochemical and hydrologic conditions specific to YM. Understanding of geochemical processes that influence RT may be used to compensate for uncertainties in hydrologic models of the YM system (Simmons et al., 1995). Establishing the degree to which these processes are affected by changes in chemistry along transport paths will help to reasonably bound rates of RT and reductions in radionuclide concentrations.

The KTI on RT addresses the main issue identified in the DOE RSS that radionuclide concentration will be reduced during RT. In the draft issue resolution and status report (IRSR) for the RT KTI (Nuclear Regulatory Commission, 1998), this main point has been divided into four subissues: (i) identifying and evaluating processes affecting RT through fractures, (ii) identifying and evaluating processes affecting RT through porous media, (iii) identifying and evaluating processes affecting radionuclide transport through alluvium, and (iv) criticality related to transport.

The purpose of this report is to outline an approach to incorporate geochemical models in estimating sorption coefficients ($K_D$) for RT through the alluvium at YM and to demonstrate how this approach may be implemented in PA. The focus is to identify geochemical parameters that exert the most control on radionuclide sorption. Then, develops an approach that incorporates sorption dependence on these parameters and lends itself to the abstraction processes for PA of the proposed repository. Existing geochemical sorption models have been used to refine sorption response surfaces that will allow sampling of water chemistry parameters and determination of radionuclide $K_D$s for incorporation into PA transport models. Site-specific data are assumed to bound alluvium water chemistry and are used to develop probability distribution functions (PDFs) of key geochemical parameters. These PDFs are used in a preliminary demonstration of how the response surfaces can be incorporated in PA.

# 2 SORPTION MODELING APPROACHES

Experimental and modeling studies of actinide sorption indicate that sorption behavior is strongly dependent on several physical and chemical properties along potential transport paths, including pH, surface area, and equilibrium $PCO_2$. Current PA abstractions do not explicitly account for changes in chemistry. To improve these abstractions, it may be possible to use geochemical sorption models to extrapolate beyond the experimental data, creating a response surface that characterizes radionuclide sorption as a function of these parameters. The approach presented here does not predict changes in geochemical conditions at YM, but it is not dependent on a single set of parameters and can be readily adapted as constraints on the geochemical environment are refined.

## 2.1 KEY GEOCHEMICAL PARAMETERS

The sorption coefficient ($K_D$) is a convenient representation of sorption data and is commonly used to represent retardation in transport models used in PA. The $K_D$ (mL/g) can be defined as:

$$K_D \text{ (mL/g)} = \frac{\text{equilibrium mass of radionuclide sorbed on solid}}{\text{equilibrium mass of radionuclide in solution}} \times \left(\frac{V}{M}\right) \qquad (2\text{-}1)$$

where V is the volume of experimental solution in mL and M is the mass of solid in g. The use of $K_D$ has the effect of normalizing sorption data to the solid-mass to solution-volume (M/V) ratio used in laboratory batch experiments and provides a means of accounting for the change in solution concentration that occurs during the course of the experiment. Results are presented in the following sections in terms of $K_D$ versus pH or in terms of $K_{A'}$ (mL/m$^2$) versus pH, where $K_{A'}$ is $K_D$ normalized to the mineral's effective specific surface area ($A'$) (i.e., $K_{A'} = K_D/A'$).

In PA studies, contaminant sorption is typically modeled assuming a $K_D$ PDF for a given radionuclide for each hydrostratigraphic unit (e.g., Wilson et al., 1994; TRW Environmental Safety Systems, Inc., 1995; Wescott et al., 1995). This approach is readily incorporated into existing transport codes and simplifies the numerical simulation of radionuclide migration. Experimental results, however, show a link between the aqueous speciation of an actinide and its sorption behavior (Pabalan et al., 1998; Bertetti et al., 1998). The similarity in the pH-dependence of actinide sorption on a wide variety of minerals such as quartz, α-alumina, clinoptilolite, montmorillonite, amorphous silica, kaolinite, and titanium oxide, which are substrates of distinct surface charge properties, suggests that actinide sorption is not sensitive to the surface charge characteristics of the sorbent as compared to the effect of changing the total number of available sites. The experimental and modeling results demonstrate that changing M/V has little influence on actinide sorption, except at low values. Ionic strength effects are limited for actinide surface complexation reactions, although these effects can be important if ion exchange is the predominant sorption mechanism. Data derived from the literature suggest that the magnitudes of actinide sorption (at a specific pH, initial radionuclide concentration, and $PCO_2$) are the same for different minerals if normalized to an A′ (Bertetti et al., 1998; Pabalan et al., 1998) (figure 2-1).

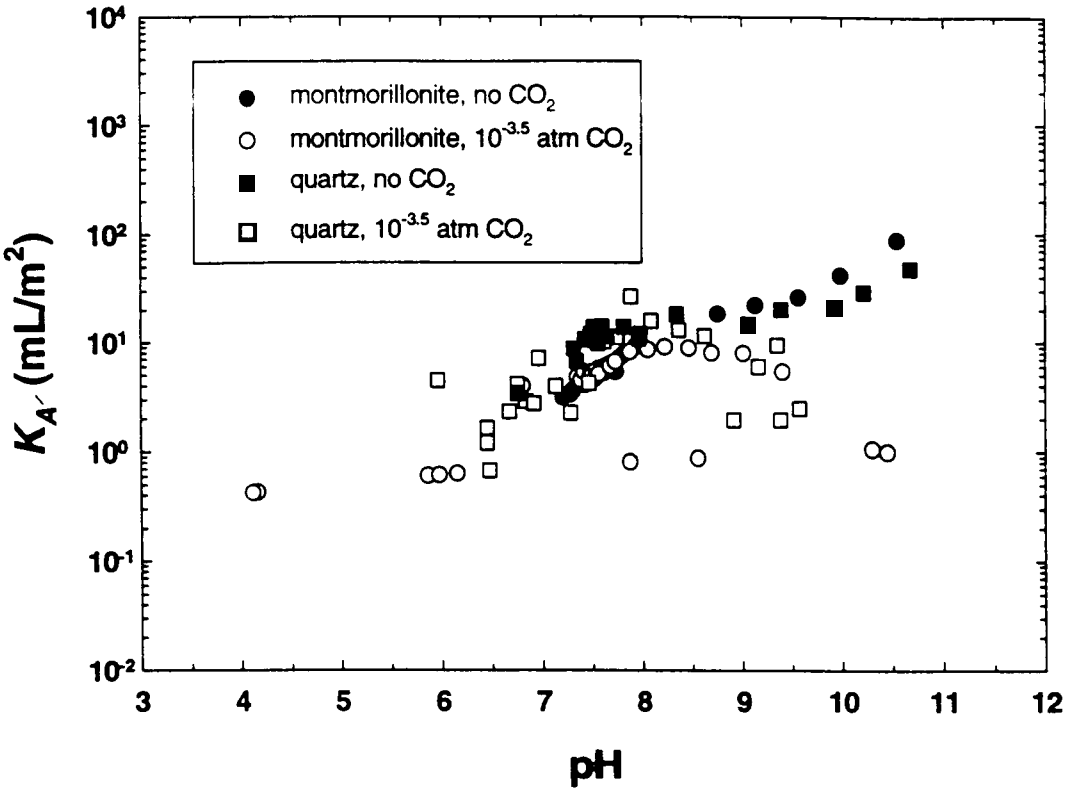


**Figure 2-1. Np(V) sorption data for montmorillonite and quartz plotted as a function of $K_{A'}$ under $CO_2$-free conditions (open symbols) and in equilibrium with atmospheric $CO_2$ ($PCO_2 = 10^{-3.5}$ atm, closed symbols) (Bertetti et al., 1998)**

## 2.2 SURFACE COMPLEXATION MODELING APPROACHES

The strong pH dependence observed in sorption experiments suggests that sorption modeling should account for changing physicochemical conditions on actinide aqueous speciation and sorption. Although actinide sorption appears relatively insensitive to surface charge, a class of models that has been used with success in modeling pH-dependent sorption is the electrostatic surface complexation model (SCM) (Davis and Leckie, 1978; Westall and Hohl, 1980; Davis and Kent, 1990; Hayes et al., 1991; Turner, 1995).

### 2.2.1 Model Description

SCMs are based on the assumption of analogous behavior between aqueous complex formation in the bulk solution and formation of surface complexes with functional binding sites at the mineral-water interface. Surface reactions are written for sorbing species and mass action and mass balance relations are used to determine sorption at the mineral surface as a function of system chemistry. Of the different SCMs, the Diffuse-Layer Model (DLM) is perhaps the simplest, using a two-layer representation of the mineral-water interface. The pH dependence of surface charge development is accounted for in the DLM, but in contrast to more complex multilayer models, the DLM assumes that supporting electrolytes such as $Na^+$ and $Cl^-$ do not interact with the surface. For this reason, the DLM neglects the possible formation of outer-sphere complexes involving the background electrolytes and does not specifically address the effects of ionic strength on sorption except through the charge-potential relationship (Davis and Kent, 1990; Dzombak and

Morel, 1990). The details of the DLM and the simplified approach used in this study are described elsewhere (Davis and Kent, 1990; Dzombak and Morel, 1990; Turner and Sassman, 1996) and only a brief overview of the DLM as applied to neptunium sorption is presented here.

A generalized pH-dependent sorption reaction between aqueous actinides and a variably charged surface sorption site can be represented by Np(V) and written

$$>XOH^{\circ} + pNpO_2^{+} + nH_2O \leftrightharpoons [>XOH_q\text{-}(NpO_2)_p(OH)_n]^{p+q-n-1} + (1+n-q)H^{+} \qquad (2\text{-}2)$$

where q is the protonation state of the sorption site (q = 0, 1, or 2 for deprotonated, neutral, and protonated, respectively), and p and n are the reaction coefficients for $NpO_2^+$ and $H_2O$. $NpO_2^+$ represents the aqueous Np(V) species and $[>XOH_q\text{-}(NpO_2)_p(OH)_n]^{p+q-n-1}$ represents the Np(V) surface complex. In the SCM approach, a coulombic correction is incorporated into the mass action expressions for surface reactions to extract the intrinsic equilibrium constants (e.g., $K_+^{int}$, $K_-^{int}$ and $K^{int}_{[>XOH_q\text{-}(NpO_2)_p(OH)_n]}$) that are independent of surface charge. For sorption reactions of the type given in Eq. (2-2), is commonly referred to as the binding constant. Similar reactions can be written for other actinides such as uranium and plutonium.

The DLM has been used to simulate Np(V) sorption on montmorillonite (Turner et al., 1998). Montmorillonite is a common mineral in volcanic tuffs in the YM vicinity and is probably also present in the alluvium derived from volcanic outcrop. The observed dependence of Np(V) sorption on pH and $PCO_2$ is a consequence of mass action effects and equilibrium chemistry in the Np(V)-$H_2O$-$CO_2$-montmorillonite system represented by Eq. (2-2). In a qualitative sense, an increase in the activity of $NpO_2^+$ drives the equilibrium reaction in Eq. (2-2) forward (increasing sorption). The presence of a complexing ligand such as dissolved carbonate in a $CO_2$ atmosphere tends to form aqueous actinide-carbonate complexes in competition with the sorbing clay surface. Carbonate competition for the available actinide increases with increasing pH, reducing the aqueous activity of $NpO_2^+$ and driving the reaction in the opposite direction (decreasing sorption). This explanation is, of course, simplistic due to the synergistic effects between solution chemistry, sorption site protonation state, and speciation of the aqueous and surface complexes.

## 2.2.2 Sorption Modeling—Diffuse-Layer Model Parameters

MINTEQA2 (Allison et al., 1991), a geochemical equilibrium speciation model capable of computing equilibria among dissolved, adsorbed, and solid and gas phases, was used to simulate the sorption of Np(V) onto the surface of montmorillonite. A relatively simple two-site DLM, previously used in Turner et al. (1998), was applied to existing Np(V) experimental data. Binding constants and surface acidity constants used in the modeling were taken from those included in Turner et al. (1998) and the references contained therein. A summary of the physical and chemical conditions that remained unchanged during the model runs is given in table 2-1.

As used here, the DLM has specific limitations that may affect its applicability over a broad range of conditions, minerals, or both. First, the model parameters (i.e., binding constant and surface reactions modeled) are based on a limited number of Np(V) sorption experiments conducted over a limited range of $PCO_2$, M/V, and Np(V) concentrations. Second, the model provides for adsorption reactions only and does

**Table 2-1. Conditions and reaction constants used for the Diffuse-Layer Model in this study**

| | |
|---|---|
| Site density | 2.3 sites/nm$^2$ |
| Surface area[a] | 9.7 m$^2$/g |
| **Edge-Site Reactions** | **Log K** |
| $>AlOH^o + H^+ \rightleftharpoons >AlOH_2^+$ | 8.33[b] |
| $>AlOH^o \rightleftharpoons >AlO^- + H^+$ | -9.73[b] |
| $>AlOH^o + NpO_2^+ + H_2O \rightleftharpoons >AlO\text{-}NpO_2(OH)^- + 2H^+$ | -13.79[c] |
| $>SiOH^o \rightleftharpoons >SiO^- + H^+$ | -7.20[b] |
| $>SiOH^o + NpO_2^+ \rightleftharpoons >SiOH\text{-}NpO_2^+$ | 4.05[c] |
| **Aqueous Speciation Reactions** | **Log K** |
| $NpO_2^+ + H_2O \rightleftharpoons NpO_2OH^o + H^+$ | -10.0[d] |
| $NpO_2^+ + 2H_2O \rightleftharpoons NpO_2(OH)_2^- + 2H^+$ | -22.4[d,e] |
| $NpO_2^+ + CO_3^{2-} \rightleftharpoons NpO_2CO_3^-$ | 4.6[e,f,g] |
| $NpO_2^+ + 2CO_3^{2-} \rightleftharpoons NpO_2(CO_3)_2^{3-}$ | 7.0[e,f,g] |
| $NpO_2^+ + 3CO_3^{2-} \rightleftharpoons NpO_2(CO_3)_3^{5-}$ | 8.5[f,g] |
| $NpO_2^+ + NO_3^- \rightleftharpoons NpO_2NO_3^o$ (aq) | -0.5[h] |

[a]Effective edge site surface area assumed to be 10 percent of total $N_2$-BET surface area (97 m$^2$/g). See text for detailed discussion.
[b]Acidity constants for am-$SiO_2$ and α-$Al_2O_3$ from Turner and Sassman (1996)
[c]Np(V)-montmorillonite binding constants from Turner et al. (1998)
[d]Lemire and Garisto (1989)
[e]Fuger (1992)
[f]Lemire (1984)
[g]Lemire et al. (1993)
[h]Danesi et al. (1971)

not consider any ion exchange reactions. Ion exchange is not considered because the experiments on which the model is based were conducted at relatively high ionic strength in an effort to suppress ion exchange in the montmorillonite at low pH. Thus, the extent of chemical and physical conditions over which the model can be applied should be carefully considered.

Since Np(V) sorption is known to be sensitive to a variety of system physicochemical conditions, several model simulations were conducted to assess the sensitivity of the model to system variables. Simulations were conducted over a range of pH, $PCO_2$, M/V, and Np(V) concentration. A summary of all MINTEQA2 model runs is provided in table 2-2.

In general, for each model simulation, $PCO_2$ was held constant while pH was varied throughout a range from 2 to 11.75. During each run, MINTEQA2 solves the equilibrium chemistry model for the specific set of conditions applied and produces sorption results for the species of interest. MINTEQA2 reports percent

10/25

**Table 2-2. Summary of MINTEQA2 simulations**

| Run | pH range | $PCO_2$ (atm) | $Np(V)_{total}$ | M/V (g/L) |
|---|---|---|---|---|
| 1 | 2 to 11.75 in 0.25 increments | no $CO_2$, $10^{-7}$ through $10^{-2}$ atm in $10^{0.5}$ atm increments | $8.9 \times 10^{-7}$ M | 4 |
| 2 | 2 to 11.75 in 0.25 increments | no $CO_2$, $10^{-7}$ through $10^{-2}$ atm in $10^{0.5}$ atm increments | $2.0 \times 10^{-11}$ M | 4 |
| 3 | 2 to 11.75 in 0.25 increments | no $CO_2$, $10^{-7}$ atm, $10^{-3.5}$ atm | $8.9 \times 10^{-7}$ M | 40 |
| 4 | 2 to 11.75 in 0.25 increments | no $CO_2$, $10^{-7}$ atm, $10^{-3.5}$ atm | $8.9 \times 10^{-7}$ M | 400 |
| 5 | 2 to 11.75 in 0.25 increments | no $CO_2$, $10^{-7}$ atm, $10^{-3.5}$ atm | $8.9 \times 10^{-7}$ M | 2,000 |
| 6 | 2 to 11.75 in 0.25 increments | no $CO_2$, $10^{-7}$ atm, $10^{-3.5}$ atm | $1.0 \times 10^{-14}$ M | 4 |
| 7 | 2 to 11.75 in 0.25 increments | no $CO_2$, $10^{-7}$ atm, $10^{-3.5}$ atm | $1.0 \times 10^{-18}$ M | 4 |

Np(V) remaining in solution and percent Np(V) sorbed on surface sites. These values are then converted to $K_D$ and, subsequently, $K_A$'s by applying the known conditions [Np(V) concentration, M/V, and surface area of the mineral] of the model run. As previously shown in figure 2-1, $K_A$ values (normalized to mineral surface areas) are useful for comparing the sorption of Np(V) onto different minerals. One major advantage of the normalization is that a $K_D$ for any specific mineral can be calculated given only the mineral's measured surface area.

Following the simulations, generated data were analyzed to identify important variables and evaluate significant trends and consistencies. Surface plots of results were generated. An effort was then made to evaluate the best approach to reproducing the sorption coefficient or response surface.

### 2.2.3 Modeling Results

The SCM results were compared to existing experimental data in an effort to confirm the validity of the simulations. A comparison of the SCM generated data with experimental data collected under similar Np(V) concentration, M/V and over a range of pH and $PCO_2$ confirms that the model capably reproduces the data on which it is based (figure 2-2).

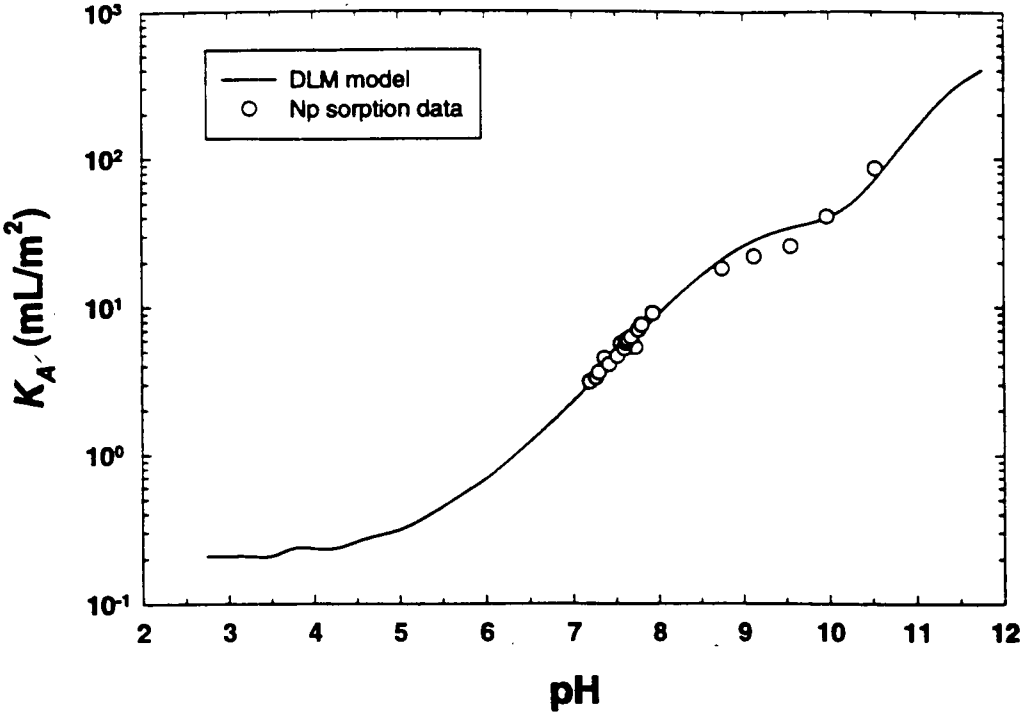


**Figure 2-2. Comparison of Diffuse-Layer Model output versus experimental data for Np(V) sorption onto montmorillonite under $CO_2$-free conditions. $Np(V)_{total}$ ~ 1 x $10^{-6}$ M, M/V = 4 g/L**

### 2.2.3.1 Sensitivity of the Model to Variation in pH

As previous experimental results demonstrate, Np(V) sorption is sensitive to solution pH. The DLM used in this study reproduces the pH dependency well (figure 2-3). In general, Np(V) sorption follows a trend similar to the hydrolysis of the $NpO_2^+$ species in solution (Bertetti et al., 1996). The dependence of Np(V) sorption on solution pH is significant. For any set of additional variables [e.g., $PCO_2$, M/V, Np(V) concentration], there is a distinct increase in sorption with increasing pH starting at pH~6. For simulations where $CO_2$ is present, Np(V) sorption continues to increase with increasing pH, eventually peaking between pH 7.5 and pH 10. Under $CO_2$-free conditions, Np(V) sorption continues to increase throughout the simulated pH range up to pH 11.75. For $PCO_2$ greater than zero, Np(V) sorption decreases with increasing pH after reaching its maximum until it finally attains a calculated value of zero at high pH values. The actual value is dependent on the $PCO_2$ used in the model run.

### 2.2.3.2 Sensitivity of the Model to Variation in $PCO_2$

The $PCO_2$ in the model system also has a significant effect on the pH range and magnitude of Np(V) sorption (figure 2-3). The pH range of the sorption envelope [the region where sorption of Np(V) increases, rises to a maximum, and then decreases] decreases as the $PCO_2$ increases. The peak (maximum magnitude) of Np(V) sorption occurs at progressively lower pH values as the $PCO_2$ increases. The sorption peak shifts from pH~10.5 for $PCO_2 = 10^{-7}$atm to pH~7.5 for $PCO_2 = 10^{-2}$atm. In addition, the magnitude of the sorption maximum decreases from about 40 mL/m$^2$ for $PCO_2$ of $10^{-7}$ atm to less than 5 mL/m$^2$ for $PCO_2$ of $10^{-2}$ atm.

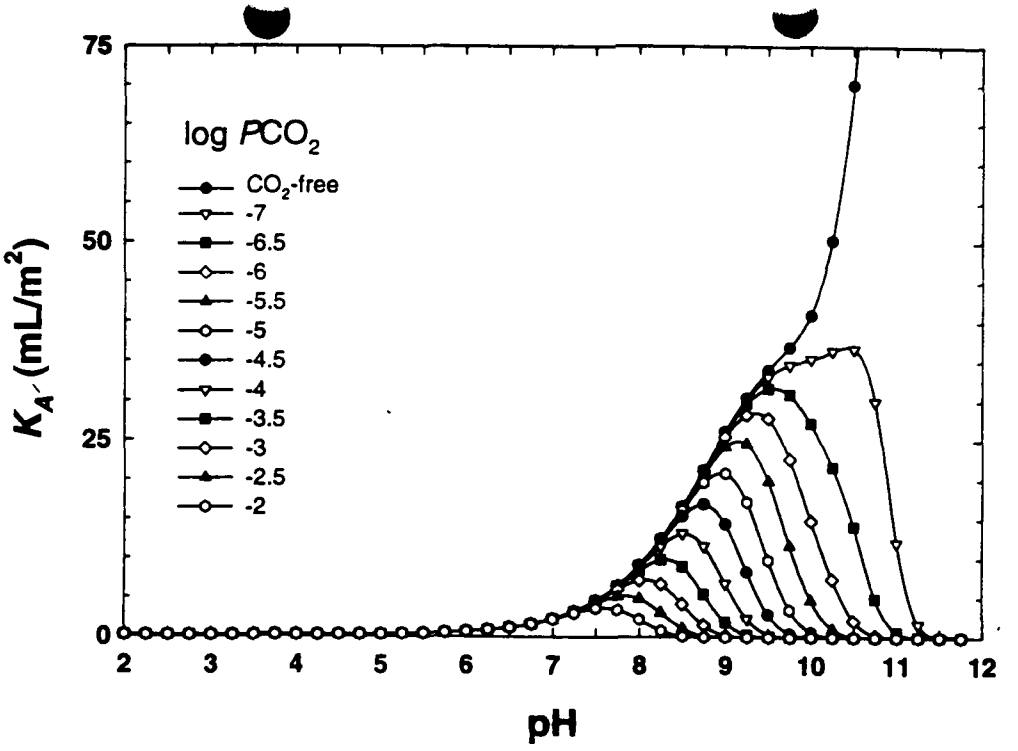


**Figure 2-3. Diffuse-Layer Model results of Np(V) sorption plotted over a range of $PCO_2$ and pH. $Np(V)_{total} \sim 1 \times 10^{-6}$ M, M/V = 4 g/L**

In fact, for any given pH within the sorption envelope, the Np(V) sorption declines exponentially with an increase in $PCO_2$ (figure 2-4). This behavior is not surprising because the $PCO_2$ is increasing exponentially and Np(V) sorption is linked to Np(V) speciation, including the formation of Np-carbonate species in solution. The results are consistent with previous experimental results (Bertetti et al., 1998; Turner et al., 1998). The model, however, slightly underpredicts sorption at higher pH when $CO_2$ is present. This may be owing to a lack of consideration of the sorption of Np-carbonate complexes or an overestimate of the presence of Np-carbonate complexes in solution (Turner et al., 1998).

### 2.2.3.3 Sensitivity of the Model to Variation in M/V

The effects of varying M/V over a range of 4, 40, 400, and 2,000 g/L are shown in figure 2-5. The model does not appear to be sensitive to changes in M/V when data is represented in terms of $K_{A'}$. That is to be expected because calculation of $K_D$, and subsequently $K_{A'}$, normalizes data for differences in M/V. It is interesting to note, however, that even a large M/V does not significantly impact the model prediction for Np(V) sorption, except at high pH with no $CO_2$ present. This has significant implications for application of this approach to field conditions where M/V is difficult, if not impossible, to determine. Essentially, if equilibrium chemical conditions are assumed, the pathway for transport (i.e., matrix or fracture flow) is then independent of the sorption model. Unfortunately, there has been little research investigating actinide sorption at widely varying M/V conditions making direct comparisons to experimental data difficult.

### 2.2.3.4 Sensitivity of the Model to Variation in Np(V) Concentration

Neptunium concentration was varied over a range of 12 orders of magnitude from $10^{-6}$ to $10^{-18}$ M. Nevertheless, the predicted Np(V) sorption was similar over the range of pH and $PCO_2$ modeled

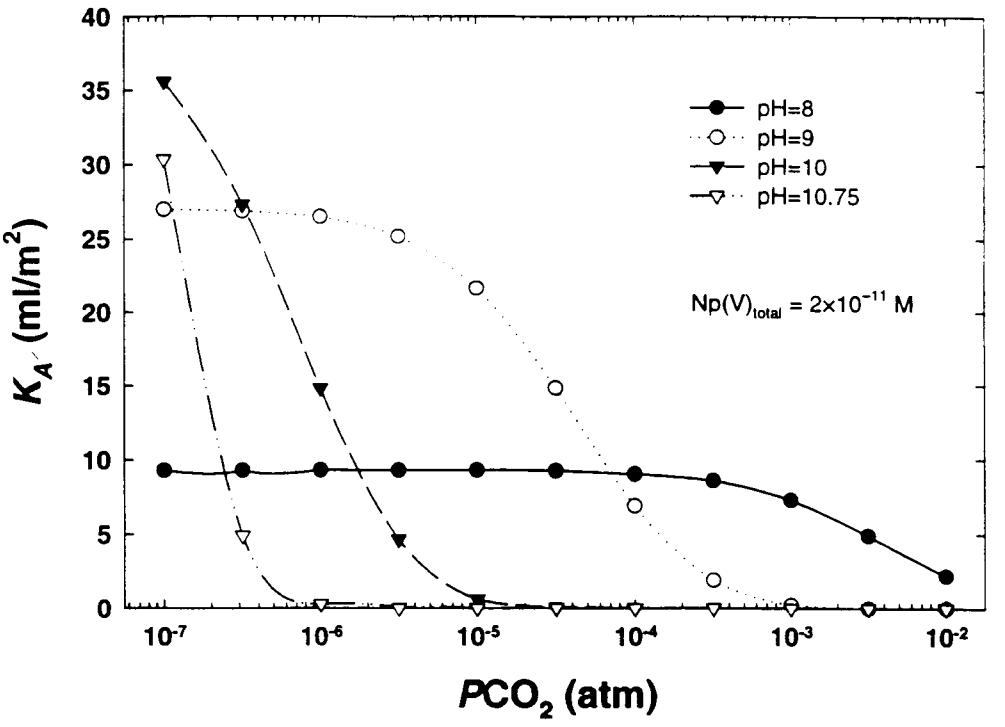


**Figure 2-4. Diffuse-Layer Model results showing a decrease in Np(V) sorption as a function of $PCO_2$ for given pH values. $Np(V)_{total} \sim 2 \times 10^{-11}$ M, M/V = 4 g/L**

(figure 2-6).These model results agree with experimentally derived results of Np(V) sorption at varying Np(V) concentrations (e.g., Righetto et al., 1991; Bertetti et al., 1998), although those studies were conducted over a much smaller range of concentrations. Experimental studies over a broad range of concentration are difficult to conduct because of the difficulty in analyzing Np(V) over that range. Because of varying experimental conditions, it is often difficult to compare between experiments. A lack of model sensitivity to changes in Np(V) concentration is significant because it implies that the model does not have to be modified to account for loss of Np(V) through sorption when expressed as $K_D$ or $K_A$ rather than percent sorbed. Therefore, no re-evaluation of $K_D$s would be required in PA because of changes in Np(V) concentration. Only changes in pH and $PCO_2$ would need to be considered.

In conclusion, the DLM of Np(V) sorption appears sensitive only to changes in pH and $PCO_2$. Thus, a single model surface can be constructed that covers a range of pH and $PCO_2$. Figure 2-7 depicts a 3-dimensional representation of the response surface using an M/V of 4 g/ L and Np(V) concentration of $\sim 1 \times 10^{-6}$ M. The Np(V) sorption envelope (region where Np(V) sorption is significant) begins at about pH 6 and extends to pH 10.5 for $PCO_2$ of $10^{-7}$ atm. For $CO_2$-free conditions, the Np(V) sorption continues to increase as pH increases. The envelope shrinks as $PCO_2$ increases so that at $PCO_2$ of $10^{-2}$ atm, the pH range of sorption is from pH 6 to pH 8.5. A sorption edge can be defined as the pH range where the magnitude of sorption changes from minimum to maximum. Within this report, the low pH sorption edge is defined as the pH range where sorption increases with increasing pH, while the high pH sorption edge is defined as the pH

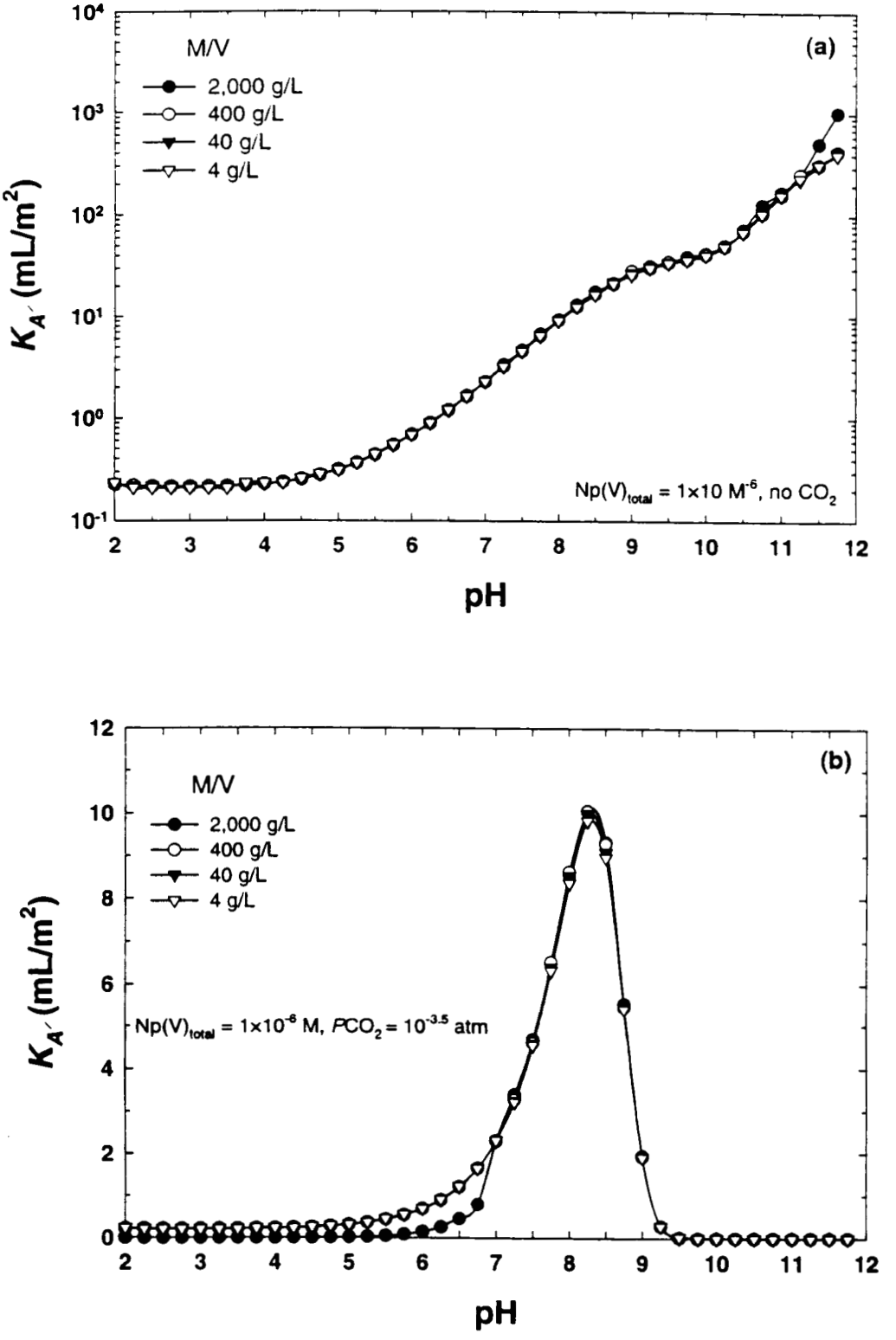


**Figure 2.5. Diffuse-Layer Model results for Np(V) sorption at various M/V values under (a) $CO_2$-free conditions and (b) atmospheric $CO_2$ ($PCO_2 = 10^{-3.5}$ atm). $Np(V)_{total} \sim 1 \times 10^{-6}$ M**

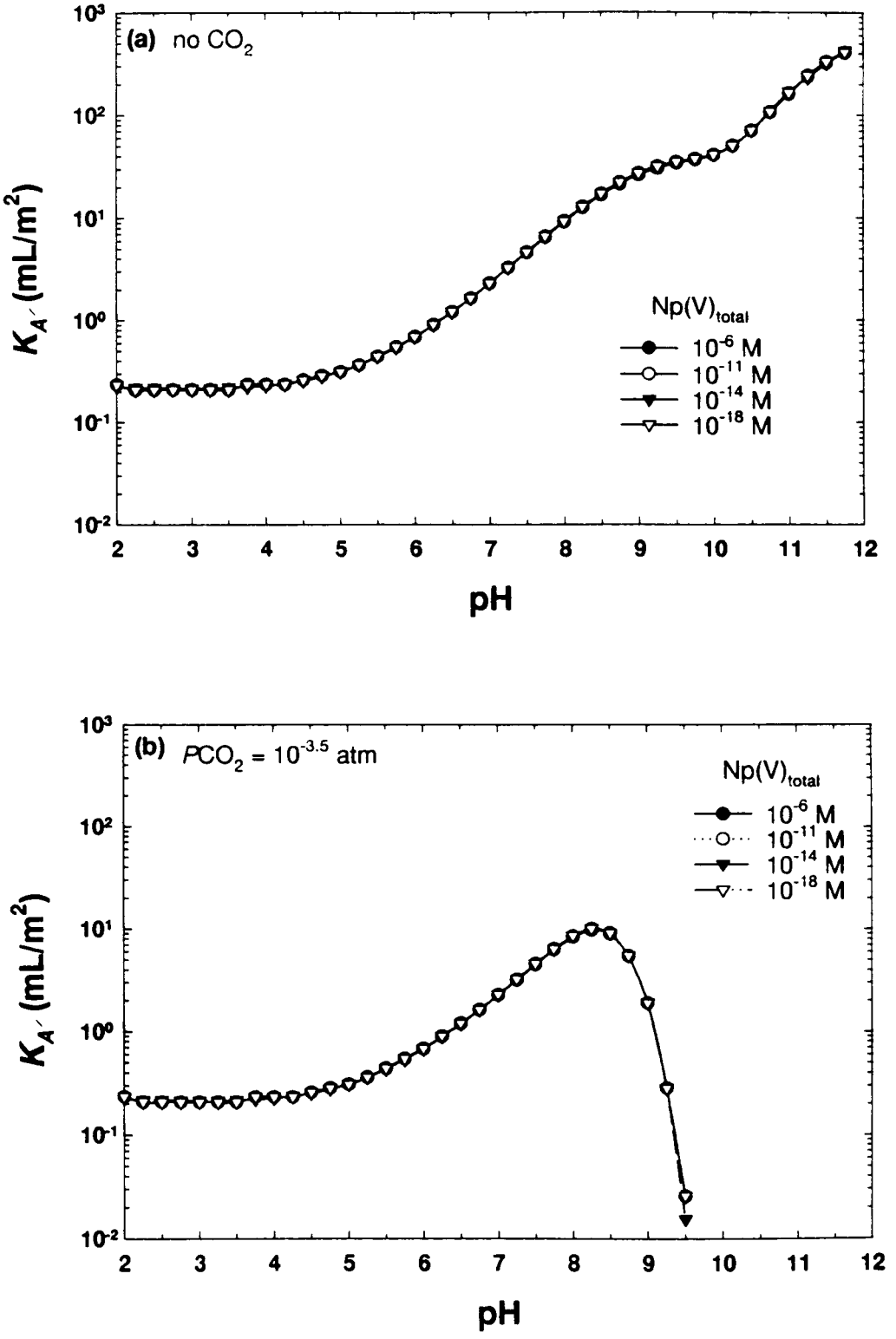


**Figure 2-6. Diffuse-Layer Model results for Np(V) sorption at various Np(V) concentrations under (a) $CO_2$-free conditions and (b) atmospheric $CO_2$ ($PCO_2 = 10^{-3.5}$ atm). M/V = 4 g/L**

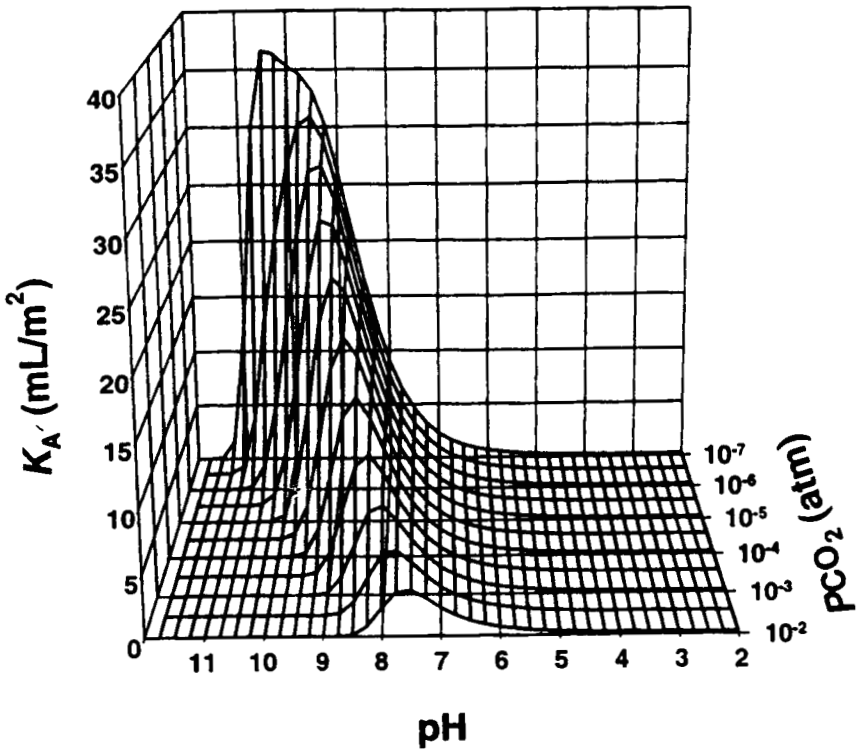


**Figure 2-7. Response surface for Np(V) sorption calculated using the Diffuse-Layer Model. Data are plotted from $10^{-7}$ to $10^{-2}$ atm ($CO_2$-free results not shown for clarity). $Np(V)_{total} \sim 1 \times 10^{-6}$ M, M/V = 4 g/L**

region where Np(V) sorption decreases with increasing pH. Note that for Np(V) sorption on montmorillonite, the envelope is asymmetrical, with the high pH sorption edge usually having a steeper slope than the low pH sorption edge, especially at low $PCO_2$.

## 2.2.4 Comparison of the Sorption Model to Experimental Data

If the response surface modeled in this study is to be successfully included as part of the total system performance assessment (TPA) code, it must be validated with reproducible experimental data collected under similar solution chemistries. Comparisons to data generated in experiments conducted at the Center for Nuclear Waste Regulatory Analyses (CNWRA) using a variety of minerals (Bertetti et al., 1998; Turner et al., 1998) reveal that the model performs favorably over a limited range of pH, M/V, Np(V) concentration, and $PCO_2$ (figure 2-8).

Additional data, however, must be considered to extend the range of applicability. (Please note that this comparison is preliminary and provided as a scoping analysis only. The comparison is not intended to be comprehensive nor meant as a critique of the methods or accuracy of the peer-reviewed experiments and data included.) To be broadly applicable or uniformly the $K_{A'}$ model should be capable of representing a spectrum of conditions and a number of mineral or rock types. Unfortunately, comparison of experimental data is difficult because of the wide range of experimental conditions, mineral preparation techniques, and differences in methods used for Np(V) analyses. Assuming the model presented here is correct in its representation of independence with respect to changes in Np(V) concentration and M/V, and since pH is generally reported, only the $PCO_2$ and mineral surface area need be known to produce a comparison between

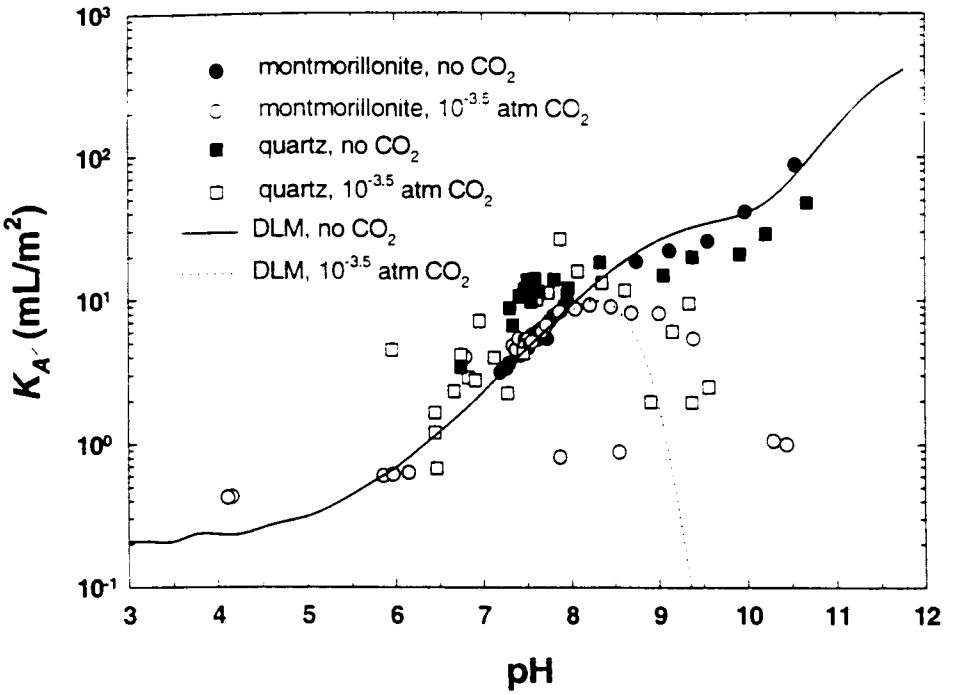


**Figure 2-8. Diffuse-Layer Model results for Np(V) sorption versus Center for Nuclear Waste Regulatory Analyses experimental Np(V) sorption data (Bertetti et al., 1998) for montmorillonite and quartz**

experiments. Even the mineral surface area may vary significantly depending on the methods used to determine surface area. For instance, surface area measurements of montmorillonite using ethylene glycol often produce estimated surface areas of 600 $m^2/g$, whereas measurements of montmorillonite using the BET-$N_2$ adsorption method produce estimated surface areas closer to 100 $m^2/g$.

Appropriate experimental data to examine include a mix of minerals (such as montmorillonite and quartz), have been conducted at different Np(V) concentrations, or have some variance in $PCO_2$. Data from several studies (Beall and Allard, 1981; Torstenfelt et al., 1988; Righetto et al., 1991; Legoux et al., 1992) are plotted with the model curves for $CO_2$-free conditions and $PCO_2$ of $10^{-3.5}$ atm in figures 2-9 and also $10^{-7}$ atm in figure 2-10. A summary of the experimental conditions is given in table 2-3.

Data from Legoux et al. (1992) include BET surface area measurements and correlate well with the model $K_{A'}$ plot (figure 2-10). The minerals used by Legoux et al. (1992) are mixtures of quartz and clay. Data from Righetto et al. (1991) were collected at $Np(V)_{total} \sim 10^{-14}$ M on colloidal silica. No surface area measurements are available for the colloid, but Righetto et al. (1991) report 1 μm-sized aggregates of particles. Assuming the average spherical particle size was 50 nm, a reasonable calculated surface area for the colloids would be 20 $m^2/g$. This results in a favorable comparison of the Righetto et al. (1991) data to the model data (figure 2-10). Data from Beall and Allard (1981) include experiments using both montmorillonite and quartz at $Np(V)_{total} \sim 2 \times 10^{-11}$ M. Data from the quartz experiments have high $K_D$ (figure 2-9) and it is difficult to assume a surface area that might result in $K_{A'}$s equivalent to the model. There is little information,

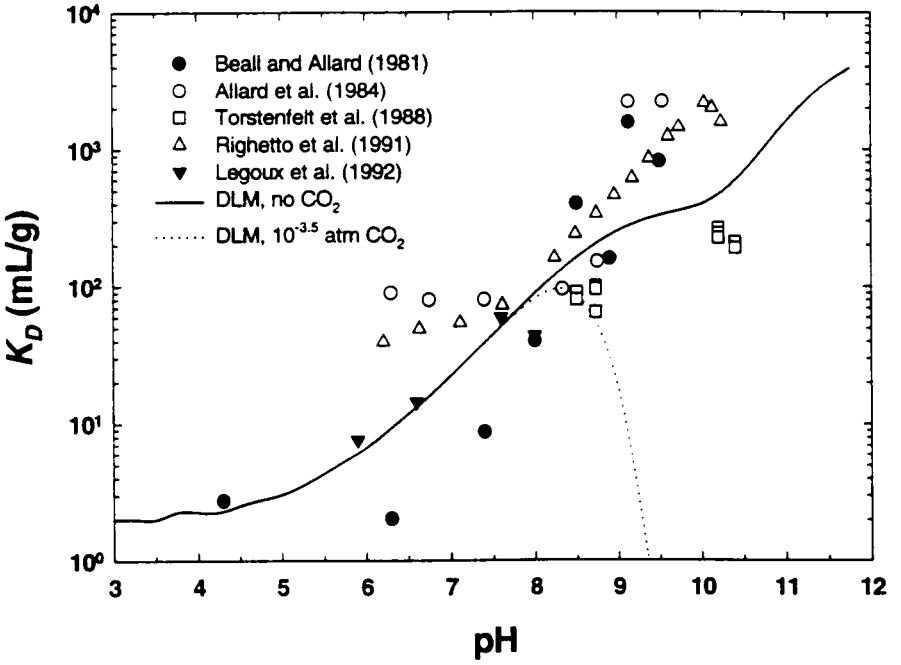


**Figure 2-9. Diffuse-Layer Model results for Np(V) sorption plotted versus data from other experimental studies. Minerals include quartz (Beall and Allard, 1981); montmorillonite (Allard et al., 1984); illite and bentonite (Torstenfelt et al., 1988); colloidal silica (Righetto et al., 1991); quartz-clay mixture (Legoux et al., 1992)**

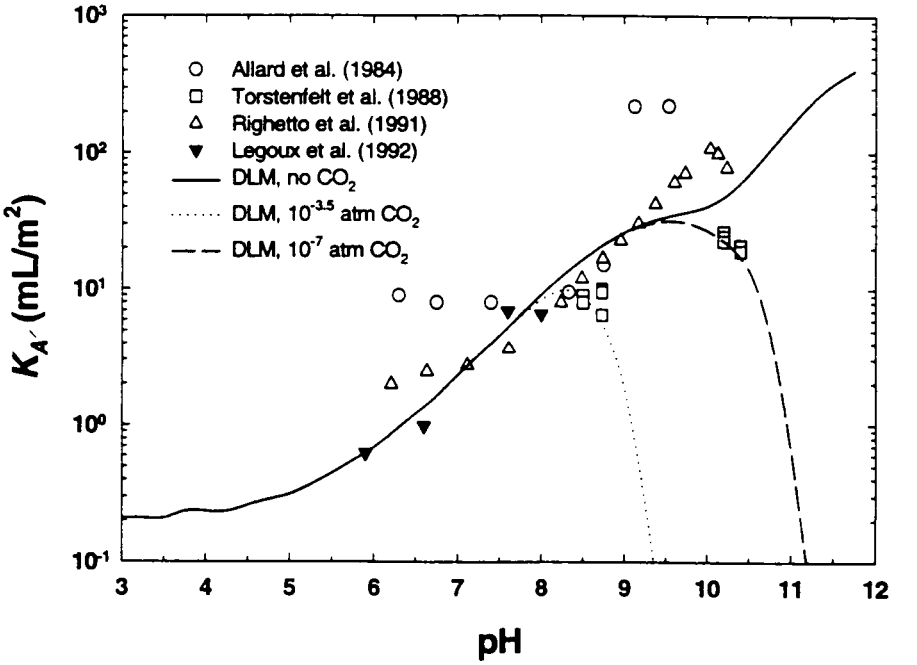


**Figure 2-10. Diffuse-Layer Model results for Np(V) sorption plotted versus $K_{A'}$ data from other studies. Data from Allard et al. (1984) and Righetto et al. (1991) are based on an estimated A′ for montmorillonite of 10 m$^2$/g (10 percent of a total $N_2$-BET surface area of about 100 m$^2$/g)**

**Table 2-3. Summary of experimental conditions for data used as comparison to DLM**

| Investigators | Conditions |
|---|---|
| Beall and Allard (1981) | $Np(V)_{total}$~2 x $10^{-11}$ M, quartz |
| Allard et al. (1984 ) | $Np(V)_{total}$~2 x $10^{-11}$ M, montmorillonite |
| Torstenfelt et al. (1988) | $Np(V)_{total}$<$10^{-7}$ M, illite and bentonite, pH~8 and ~10, 143 ppm $HCO_3^-$ |
| Righetto et al. (1991) | $Np(V)_{total}$<$10^{-14}$ M, colloidal silica, pH 2-10, no specified $CO_2$ conditions (appear $CO_2$-free) |
| Legoux et al. (1992) | $Np(V)_{total}$~5 x $10^{-12}$ M, mix of quartz, smectite, glauconite, kaolinite. Measured $N_2$-BET surface area, 2.1 - 52.4 ppm $CO_3^{2-}$ |

however,on the mineral preparation for quartz used in the Beall and Allard (1981) studies. If the quartz surfaces were contaminated with Fe-oxides, even in small quantities, the resulting $K_D$s would be larger than those expected for a pure quartz sorbent. Beall and Allard (1981) also report bicarbonate concentrations of 90–275 mg/L. No effect of reduction in sorption because of the presence of carbonate is revealed in their Np(V) sorption results. The trend of a decrease in Np(V) sorption with increasing pH due to the presence of carbonate has been reported by several other investigators (e.g., Meyer et al., 1985; Righetto et al., 1991; and Bertetti et al., 1998). Data from Allard et al. (1984) for montmorillonite also show high $K_D$s and little or no influence of the presence of carbonate. If a surface area of 100 $m^2/g$ is assumed (A′ of 10 $m^2/g$) for the Allard et al. (1984) montmorillonite, their data correlate better with the model used here, although $K_{A'}$s are still greater than the model prediction at high pH with significant sorption present, possibly because of ion exchange, at lower pH (figure 2-10). To use data from Torstenfelt et al. (1988), a surface area for the clay must also be assumed (surface area = 100 $m^2/g$ or A′ = 10 $m^2/g$). When converted to $K_{A'}$ and including the presence of $CO_2$ reported in Torstenfelt et al. (1988) experiments, their data correlate well with the model (figure 2-10).

In conclusion, the model performs adequately when compared to experimental data collected by different researchers under a variety of chemical conditions with a mixture of montmorillonite, quartz, and other clay minerals. When the model falters, it generally predicts $K_{A'}$ values lower than values measured experimentally, which is considered to be conservative with respect to PA model results. Broad applicability of the model is limited by

- A consistent underestimation of Np(V) sorption at high pH when $PCO_2$ is greater than zero
- A failure to account for ion exchange at low pH
- Difficulties in comparing data among experiments to validate the model over a wide range of conditions because of incomplete information
- An underestimation of sorption for some experimental data, although the problems listed previously may contribute greatly to this problem
- general lack of Np(V) sorption experimental data at high M/V.

15/25

# 3 APPROACHES FOR SORPTION MODELING IN PERFORMANCE ASSESSMENT

Notwithstanding the limitations of the approach, the model has potential for application as part of the TPA code. Several options for incorporation of the sorption coefficient response surface exist (see figure 2-7). First, the response surface or an interpolated version of the surface can be generated as a database or look-up table with indices of pH and $PCO_2$. Second, a mathematical representation of the response surface may be generated so that pH and $PCO_2$ could be entered into a function that would produce a $K_{A'}$ output. Finally, a combination of the look-up table and mathematical representation of the DLM-generated response surface is developed and applied using site-specific data.

## 3.1 LOOK-UP TABLE OR INTERPOLATED SURFACE

The modeled Np(V) sorption surface shown in figure 2-7 is a noninterpolated mesh consisting only of model generated data (mesh intersections). Because of the range of data produced, especially for $PCO_2$, interpolations of the surface, regardless of methods used (e.g., linear interpolation, kriging), resulted in inadequate representations of the response surface. Interpolations failed to accurately portray the model surface, even with limited data sets. MINTEQA2 and the DLM are capable of producing a data set with a point density fine enough for further processing. The only disadvantage of this method of data generation is that it is more time consuming. The data used to create the response surface can be organized into a look-up table format in a form such as the one shown in table 3-1 (or in a matrix more suitable for TPA). The look-up table would represent a simple and fast mechanism for extracting appropriate $K_{A'}$s. The primary disadvantages of the look-up table are that it requires some form of interpolation for both pH and $PCO_2$ since the data are based on discrete indices and regeneration and replacement of data are necessary if a more suitable model for $K_{A'}$ is found.

## 3.2 THREE-DIMENSIONAL MATHEMATICAL REPRESENTATION

A second approach to incorporating the $K_{A'}$ model would be to generate a mathematical representation of the DLM response surface. The mathematical model would have the advantage of using a continuous range of data without the need for interpolation. A three dimensional (3D) curve fitting application (TableCurve 3D, Jandel Scientific) was used in an attempt to mathematically model the response surface. Unfortunately, like attempts to interpolate the response surface, the curve fit routine was unable to generate a function or set of functions that adequately reproduced the response surface. The range of values to be modeled is too large for accurate reproduction over the entire data range considered. In general, the sorption maximum was underpredicted by the mathematical expressions. To improve the fit, the surface was first segregated into components to model only the range in $PCO_2$ from $10^{-7}$ to $10^{-2}$ atm, and further reduced to only the sorption range of pH 6 to 10.5. These attempts, however, were also unsuccessful in improving the results.

## 3.3 COMBINATION OF LOOK-UP TABLE AND MATHEMATICAL REPRESENTATION

Figure 3-1 provides the model results as discrete lines for each $PCO_2$ (for the figure, lines are cubic spline interpolation of the data). Based on this figure, a data set could be constructed that would require interpolation of only one component (in this example, $PCO_2$). This technique would offer the advantage of producing results over a continuous range of pH values while using information for discrete $PCO_2$ values.

**Table 3-1. Sample look-up table for Np(V) sorption response surface ($K_{A'}$ in mL/m$^2$). Np(V)$_{total}$ = $10^{-6}$ molal, M/V = 4 g/L**

| pH | Log $PCO_2$ (atm) | | | | | | | | | | | |
|---|---|---|---|---|---|---|---|---|---|---|---|---|
| | no $CO_2$ | -7.00 | -6.50 | -6.00 | -5.50 | -5.00 | -4.50 | -4.00 | -3.50 | -3.00 | -2.50 | -2.00 |
| 2.00 | 0.23407 | 0.23407 | 0.23407 | 0.23407 | 0.23407 | 0.23407 | 0.23407 | 0.23407 | 0.23407 | 0.23407 | 0.23407 | 0.23407 |
| 2.25 | 0.20785 | 0.20785 | 0.20785 | 0.20785 | 0.20785 | 0.20785 | 0.20785 | 0.20785 | 0.20785 | 0.20785 | 0.20785 | 0.20785 |
| 2.50 | 0.20785 | 0.20785 | 0.20785 | 0.20785 | 0.20785 | 0.20785 | 0.20785 | 0.20785 | 0.20785 | 0.20785 | 0.20785 | 0.20785 |
| 2.75 | 0.20785 | 0.20785 | 0.20785 | 0.20785 | 0.20785 | 0.20785 | 0.20785 | 0.20785 | 0.20785 | 0.20785 | 0.20785 | 0.20785 |
| 3.00 | 0.20785 | 0.20785 | 0.20785 | 0.20785 | 0.20785 | 0.20785 | 0.20785 | 0.20785 | 0.20785 | 0.20785 | 0.20785 | 0.20785 |
| 3.25 | 0.20785 | 0.20785 | 0.20785 | 0.20785 | 0.20785 | 0.20785 | 0.20785 | 0.20785 | 0.20785 | 0.20785 | 0.20785 | 0.20785 |
| 3.50 | 0.20785 | 0.20785 | 0.20785 | 0.20785 | 0.20785 | 0.20785 | 0.20785 | 0.20785 | 0.20785 | 0.20785 | 0.20785 | 0.20785 |
| 3.75 | 0.23407 | 0.23407 | 0.23407 | 0.23407 | 0.23407 | 0.23407 | 0.23407 | 0.23407 | 0.23407 | 0.23407 | 0.23407 | 0.23407 |
| 4.00 | 0.23407 | 0.23407 | 0.23407 | 0.23407 | 0.23407 | 0.23407 | 0.23407 | 0.23407 | 0.23407 | 0.23407 | 0.23407 | 0.23407 |
| 4.25 | 0.23407 | 0.23407 | 0.23407 | 0.23407 | 0.23407 | 0.23407 | 0.23407 | 0.23407 | 0.23407 | 0.23407 | 0.23407 | 0.23407 |
| 4.50 | 0.26034 | 0.26034 | 0.26034 | 0.26034 | 0.26034 | 0.26034 | 0.26034 | 0.26034 | 0.26034 | 0.26034 | 0.26034 | 0.26034 |
| 4.75 | 0.28666 | 0.28666 | 0.28666 | 0.28666 | 0.28666 | 0.28666 | 0.28666 | 0.28666 | 0.28666 | 0.28666 | 0.28666 | 0.28666 |
| 5.00 | 0.31303 | 0.31303 | 0.31303 | 0.31303 | 0.31303 | 0.31303 | 0.31303 | 0.31303 | 0.31303 | 0.31303 | 0.31303 | 0.31303 |
| 5.25 | 0.36595 | 0.36595 | 0.36595 | 0.36595 | 0.36595 | 0.36595 | 0.36595 | 0.36595 | 0.36595 | 0.36595 | 0.36595 | 0.36595 |
| 5.50 | 0.44572 | 0.44572 | 0.44572 | 0.44572 | 0.44572 | 0.44572 | 0.44572 | 0.44572 | 0.44572 | 0.44572 | 0.44572 | 0.44572 |
| 5.75 | 0.55285 | 0.55285 | 0.55285 | 0.55285 | 0.55285 | 0.55285 | 0.55285 | 0.55285 | 0.55285 | 0.55285 | 0.55285 | 0.55285 |
| 6.00 | 0.68799 | 0.68799 | 0.68799 | 0.68799 | 0.68799 | 0.68799 | 0.68799 | 0.68799 | 0.68799 | 0.68799 | 0.68799 | 0.68799 |
| 6.25 | 0.90713 | 0.90713 | 0.90713 | 0.90713 | 0.90713 | 0.90713 | 0.90713 | 0.90713 | 0.90713 | 0.90713 | 0.90713 | 0.90713 |
| 6.50 | 1.21444 | 1.21444 | 1.21444 | 1.21444 | 1.21444 | 1.21444 | 1.21444 | 1.21444 | 1.21444 | 1.21444 | 1.21444 | 1.18621 |
| 6.75 | 1.64510 | 1.64510 | 1.64510 | 1.64510 | 1.64510 | 1.64510 | 1.64510 | 1.64510 | 1.64510 | 1.64510 | 1.64510 | 1.64510 |
| 7.00 | 2.30218 | 2.30218 | 2.30218 | 2.30218 | 2.30218 | 2.30218 | 2.30218 | 2.30218 | 2.30218 | 2.27163 | 2.27163 | 2.24115 |
| 7.25 | 3.25067 | 3.25067 | 3.25067 | 3.25067 | 3.25067 | 3.25067 | 3.21803 | 3.21803 | 3.21803 | 3.21803 | 3.15295 | 2.99153 |
| 7.50 | 4.58393 | 4.58393 | 4.58393 | 4.58393 | 4.58393 | 4.58393 | 4.58393 | 4.58393 | 4.54821 | 4.47703 | 4.23052 | 3.61471 |
| 7.75 | 6.48362 | 6.48362 | 6.48362 | 6.48362 | 6.48362 | 6.48362 | 6.48362 | 6.44330 | 6.32294 | 6.00633 | 5.12992 | 3.44811 |
| 8.00 | 9.10258 | 9.10258 | 9.10258 | 9.10258 | 9.10258 | 9.05545 | 9.00844 | 8.86820 | 8.36349 | 7.18486 | 4.83630 | 2.21073 |
| 8.25 | 12.46597 | 12.46597 | 12.46597 | 12.46597 | 12.40932 | 12.35283 | 12.12856 | 11.47131 | 9.82514 | 6.68675 | 3.05588 | 0.79711 |
| 8.50 | 16.54732 | 16.54732 | 16.54732 | 16.54732 | 16.40879 | 16.13444 | 15.33238 | 13.15912 | 8.96157 | 4.16083 | 1.10188 | 0.10351 |
| 8.75 | 21.25818 | 21.25818 | 21.17252 | 21.08716 | 20.74882 | 19.68218 | 16.89766 | 11.57926 | 5.42922 | 1.50003 | 0.15557 | 0.00000 |
| 9.00 | 26.08434 | 25.98021 | 25.87650 | 25.46576 | 24.17486 | 20.83294 | 14.37197 | 6.80986 | 1.91015 | 0.20785 | 0.00000 | 0.00000 |
| 9.25 | 30.37756 | 30.13395 | 29.65303 | 28.25866 | 24.56508 | 17.18213 | 8.27330 | 2.36348 | 0.28666 | 0.00000 | 0.00000 | 0.00000 |
| 9.50 | 33.88698 | 33.06972 | 31.62813 | 27.80933 | 19.84308 | 9.77604 | 2.86369 | 0.33946 | 0.02580 | 0.00000 | 0.00000 | 0.00000 |
| 9.75 | 36.78310 | 34.58558 | 30.87119 | 22.67266 | 11.63347 | 3.48128 | 0.44572 | 0.02580 | 0.00000 | 0.00000 | 0.00000 | 0.00000 |
| 10.00 | 40.82421 | 35.30073 | 27.14918 | 14.75070 | 4.65561 | 0.60674 | 0.02580 | 0.00000 | 0.00000 | 0.00000 | 0.00000 | 0.00000 |

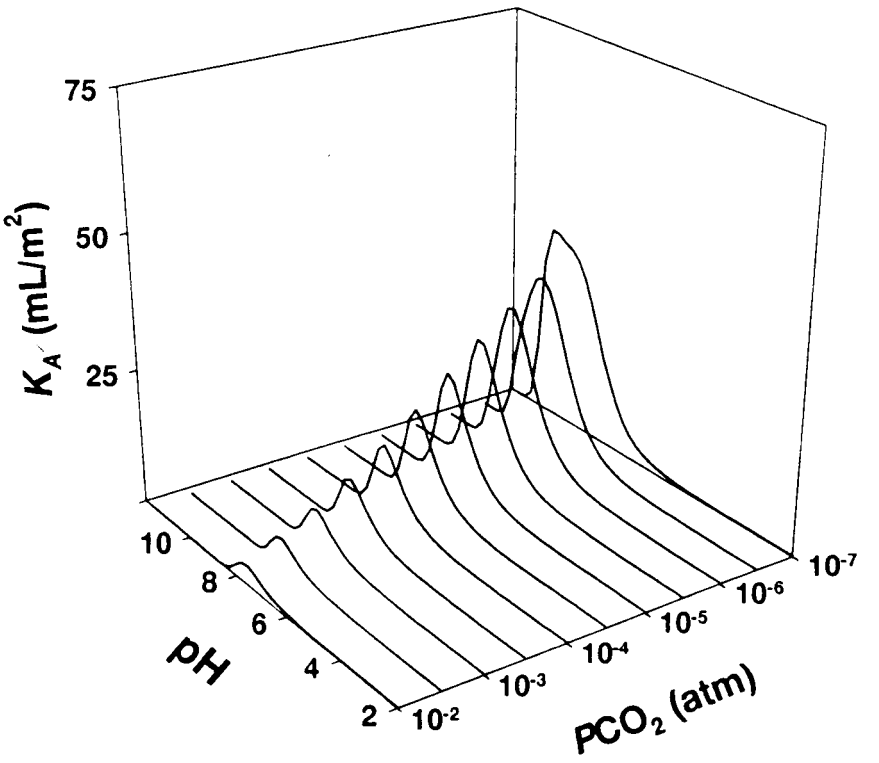


**Figure 3-1. Plot of Diffuse-Layer Model predictions of Np(V) sorption at discrete $PCO_2$ values. $Np(V)_{total} \sim 1 \times 10^{-6}$ M, M/V = 4 g/L**

The similarities in the shape of the pH curves for $PCO_2$ suggested that the same equation might be capable of representing each curve. To test this, pH-sorption curves were fit (TableCurve 2D, Jandel Scientific) to generate equations for sorption curves over a pH range appropriate for each $PCO_2$ (i.e., for $PCO_2$ of $10^{-6}$ atm the model was fit from pH 6 to pH 10; likewise, for $PCO_2$ of $10^{-2}$ atm, the model was fit from pH 6 to pH 8.5—essentially the pH range of the sorption envelope at a given $PCO_2$. $K_A$'s below pH 6 and above some pH for a given $PCO_2$ are effectively zero). A relatively simple equation.

$$\mathbf{ln(y) = a + bx + cx^2 + dx^3 + ex^4 + fx^5} \qquad (3\text{-}1)$$

(where a, b, c, d, and e are constant coefficients) was found to adequately reproduce the model predicted sorption over the desired pH range for each $PCO_2$ (including the $CO_2$-free curve). Coefficient values and goodness-of-fit values for each curve are shown in table 3-2 and sample output is graphically portrayed for selected values of $PCO_2$ in figure 3-2. Note that except for the fit of sorption at $PCO_2 = 10^{-7}$ atm, which shows some degradation at high pH, the fits are excellent. The equations are examples only and alternative equations could be inserted to improve the fit for each curve; use of one form of equation would simplify the incorporation of the model into a TPA code by requiring only a matrix for coefficients (i.e., a set for each $PCO_2$ value) and one equation. Additionally, only one parameter need be interpolated. Since pH is commonly reported, and $PCO_2$ may need conversion or calculation depending on the prevalence of available data, $PCO_2$ was left for interpolation, adjustment, or both. This method has the advantage of using a continuous range of pH data while reducing the number of discrete points needed for the look-up table.

**Table 3-2. Equation parameters and summary of fit results for model curves at discrete $PCO_2$. $Np(V)_{total} = 10^{-6}$ molal, M/V = 4 g/L**

| $PCO_2$ (atm) | Coefficients: [ln ($K_{A'}$, in mL/m$^2$) = a + bx + cx$^2$ + dx$^3$ + ex$^4$ + fx$^5$] | | | | | | | |
|---|---|---|---|---|---|---|---|---|
| | a | b | c | d | e | f | $r^2$ value | pH range used for fit |
| $10^{-2.0}$ | -323.7345029 | 151.4136753 | -17.3990293 | -1.7541185 | 0.4728224 | -0.0247745 | 0.9999 | 6–9.25 |
| $10^{-2.5}$ | -441.4872516 | 226.8171288 | -37.7488848 | 1.2089255 | 0.2378357 | -0.0167447 | 0.9999 | 6–9.25 |
| $10^{-3.0}$ | 148.2265595 | -173.8278793 | 69.4791195 | -12.8694017 | 1.1394455 | -0.0390727 | 0.9999 | 6–9.50 |
| $10^{-3.5}$ | 604.4445148 | -474.5177627 | 147.2075461 | -22.6668262 | 1.7364614 | -0.0529354 | 0.9999 | 6–9.50 |
| $10^{-4.0}$ | 847.1361569 | -620.1544804 | 180.5362481 | -26.2031203 | 1.8992944 | -0.0549789 | 0.9999 | 6–10.00 |
| $10^{-4.5}$ | 925.7298724 | -652.8079406 | 183.1897645 | -25.6433576 | 1.7939710 | -0.0501685 | 0.9999 | 6–10.25 |
| $10^{-5.0}$ | 923.2318767 | -632.0905821 | 172.1420527 | -23.3803904 | 1.5872876 | -0.0430961 | 0.9999 | 6–10.50 |
| $10^{-5.5}$ | 672.7843206 | -452.9837012 | 121.1472289 | -16.1548188 | 1.0777544 | -0.0287889 | 0.9999 | 6–11.00 |
| $10^{-6.0}$ | 393.8474607 | -258.6708687 | 67.3400912 | -8.7496479 | 0.5711094 | -0.0149989 | 0.9999 | 6–11.25 |
| $10^{-6.5}$ | 722.6946490 | -436.2310889 | 104.2139278 | -12.3723844 | 0.7340464 | -0.0174653 | 0.9978 | 6–11.50 |
| $10^{-7.0}$ | 2202.1902289 | -1290.5774270 | 299.2738666 | -34.3781522 | 1.9602212 | -0.0444424 | 0.9816 | 6–11.75 |
| no $CO_2$ | 1211.3978170 | -705.8275247 | 161.4080394 | -18.1364167 | 1.0036927 | -0.0219067 | 0.9996 | 6–11.75 |

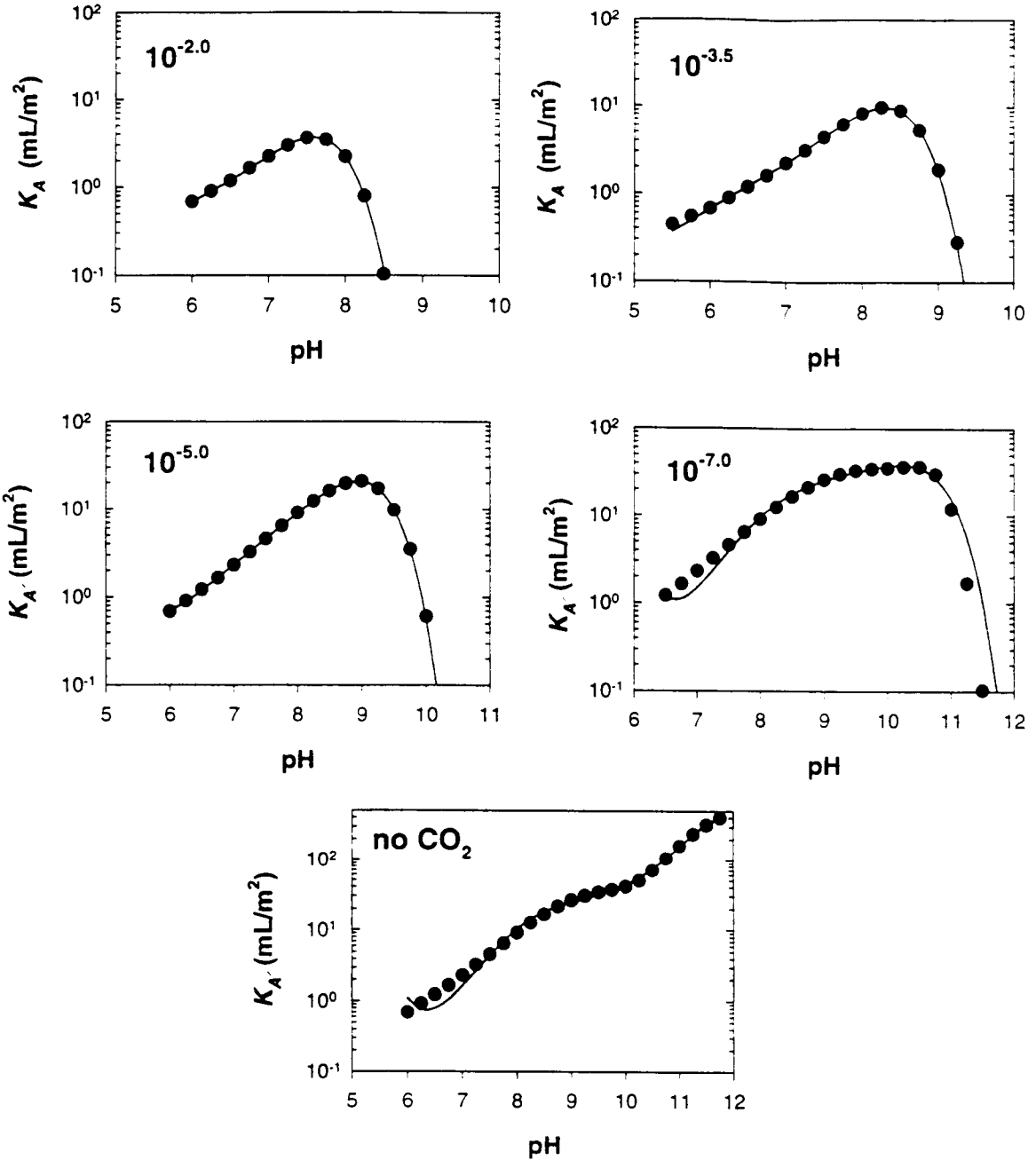


**Figure 3-2. Plots of polynomial fits to Diffuse-Layer Model $K_A$s (points) for selected discrete values of $PCO_2$. Polynomial coefficients are given in table 3-2. Values listed in the upper left-hand corner of each plot show $PCO_2$ in atm for the particular data set and fit**

# 4 TESTING THE MODEL WITH SITE-SPECIFIC INFORMATION FROM ALLUVIUM NEAR YUCCA MOUNTAIN

As discussed, sorption behavior for a given radionuclide is dependent on the physical/chemical system being studied. The approach presented in section 3 does not provide predictions of geochemical conditions at YM. It does, however, provide a means of using available information to incorporate a level of geochemical dependence and internal consistency that is lacking in current PA abstractions of sorption. Although only limited information is available on alluvium mineralogy in the YM vicinity, there is material currently accessible for site-specific groundwater chemistry. These data can be used to demonstrate how the approach outlined previously might be incorporated into PA models, but the response surface for Np(V) sorption is not limited to these data.

## 4.1 ALLUVIUM MINERALOGY

Quaternary alluvium mineralogy is not well constrained in the YM vicinity. Valley fill mineralogy typically is believed to be similar to the nearby bedrock outcrops in the watershed, depending on the degree and orientation of the valley slope (Claassen, 1985). A map of surface distribution of valley fill material is provided in Claassen (1985). In general, most of the alluvium near YM and north of the Amargosa Desert is composed of tuff and tuff detritus from the surrounding volcanic highlands, having a mineralogy similar to the original tuffs. This includes YM, Fortymile Canyon, and the drainages from Fortymile Canyon into the Amargosa Desert. Near YM, this includes the tuff units at the site and mostly is limited to the more durable welded units of the Tiva Canyon and Paintbrush Tuffs. East of Fortymile Canyon, the alluvium contains rhyolite from the Calico Hills and upper reaches of Fortymile Canyon. Alluvium in the Amargosa Desert is identified as mixed lithology of Paleozoic carbonate and clastic rocks, as well as the Tertiary volcanics. The southern and eastern borders of the Amargosa Desert will tend to be dominated by carbonate rocks because of erosion from the Funeral Mountains to the south and the Striped Hills, Skull Mountain, and the Spring Mountains to the east.

Size fractions range from clay in the valley bottoms to cobbles and boulders closer to outcrop (Cornwall, 1972). At the surface, clasts have been modified by exposure. Coatings of calcite and silica are common, as well as rock varnish consisting of manganese oxides. Additional lithologies, minor in extent but might impact transport in the alluvium, include playa deposits from evaporation in the southeastern part of the Amargosa Desert, calcrete deposits from infiltrating precipitation, and opal and calcite fillings in fractures and spring deposits (National Research Council, 1992). Clay units may also form from weathering of the alluvium, as evidenced by clay pits in Ash Meadows. A test hole drilled about 5 km southwest of Lathrop Wells indicates that playa deposits may exist at depths of more than 400 m (Claassen, 1985).

## 4.2 SATURATED ZONE GROUNDWATER CHEMISTRY

A comprehensive source of water chemistry data is found in the U.S. Geological Survey report of Perfect et al. (1995). This comprehensive dataset of over 3,700 analyses has been culled using screening criteria outlined in Turner (1998) to produce a smaller subset of complete chemical analyses (n = 460) suitable for geochemical modeling in the vicinity of YM. These include multiple analyses for the same well/spring; and attempt has yet been made to select a preferred analysis or calculate a mean water composition for a given sampling point. The water samples as recorded in Perfect et al. (1995) are typically samples integrated from a number of aquifers or producing zones. Depth to water is sometimes indicated, but the depth to the producing horizon is not generally given. Only a few samples are collected from distinct intervals isolated by packers. These data were not generally collected under a DOE-approved quality

assurance program, but are freely used here. The sources referenced in Perfect et al. (1995) should be consulted for determining quality of the data.

PA calculations rely on PDFs to describe uncertain parameters. The database described in Turner (1998) allows identification of current ranges and distribution types for key measured geochemical parameters, including pH and $PCO_2$. Descriptive statistics from Turner (1998) are included in table 4-1.

### 4.2.1 pH

As demonstrated in section 3, pH is a key parameter for controlling sorption. For the screened database described in Turner (1998) (n = 460 samples), the minimum and maximum pH are 6.3 to 9.6. A histogram and probability plot are shown in figure 4-1a. Most of the cumulative frequencies plot in a straight line suggesting a normal distribution. There is some deviation at higher pH that is mostly due to including high concentration brines from Franklin Lake Playa in the distribution. Perfect et al. (1995) noted they have not attempted to distinguish between laboratory and field pH measurements; problems due to degassing of $CO_2$ may also exist and not be readily discernible in the dataset.

### 4.2.2 Log $PCO_2$

The partial pressure of $CO_2$ is a measure of the amount of inorganic carbon in the aqueous system related to pH and $C_T$ through aqueous carbonate geochemistry. A histogram and probability plot of calculated log $PCO_2$ is given in figure 4-1b. Although there are some values below atmospheric levels [$PCO_2$(atmospheric) = $10^{-3.5}$ atm], the bulk of the groundwaters in the YM vicinity have much higher $PCO_2$, either due to soil-zone biological processes, such as root respiration or to water from Paleozoic carbonate aquifers (Murphy and Pabalan, 1994). Most of the cumulative frequencies plot in a straight line suggesting a log-normal distribution with a mean value of about $10^{-2.5}$ atmosphere, an order of magnitude greater than atmospheric values. There is a small group of samples at low $PCO_2$ that are mostly due to high chloride brines from Franklin Lake Playa and a suite of samples collected from trench sites near the Beatty low-level waste facility. Because of the link through carbonate aqueous chemistry, log $PCO_2$ and pH are expected to be correlated. A plot of log $PCO_2$ versus pH (figure 4-2) demonstrates a negative correlation, with a slope of about -0.83. This information can be used in constraining sampling these geochemical parameters for the purposes of PA.

## 4.3 EXAMPLE: USING THE RESPONSE SURFACE WITH YUCCA MOUNTAIN SITE-SPECIFIC DATA

A response surface for $K_D$ ultimately will be used with site-specific information. One means of incorporating this information is sampling of PDFs for pH and log $PCO_2$ that are based on site-specific ambient groundwater chemistry data as described in section 4.2. Because pH and log $PCO_2$ are linked through the carbonate aqueous chemistry, selection of one parameter provides constraints on the value of the other.

For the purposes of this demonstration, the sampling routine in Microsoft Excel, Version 5.0, was used to sample 460 values of pH based on the distribution statistics defined in section 4.2. The correlation between pH and log $PCO_2$ ($\rho_{PCO_2}$, pH = -0.83; figure 4-2) was then used to define a value for log $PCO_2$.

**Table 4-1. Descriptive statistics of measured groundwater chemical parameters (from Turner, 1998)**

| | pH (standard units) | Log $PCO_2$ (atm) |
|---|---|---|
| Mean | 7.83 | -2.50 |
| Standard Error | 0.02 | 0.03 |
| Median | 7.8 | -2.45 |
| Mode | 7.8 | -2.34 |
| Standard Deviation | 0.45 | 0.54 |
| Kurtosis | 1.75 | 3.73 |
| Skewness | 0.43 | -1.30 |
| Range | 3.3 | 4.31 |
| Minimum | 6.3 | -5.08 |
| Maximum | 9.6 | -0.77 |
| Count | 460 | 460 |

A simple procedure for sampling jointly normal random variables was implemented to demonstrate how correlation between pH and the common logarithm of $PCO_2$ can be used to preserve correlation among sampled $K_D$ values for selected radionuclides. Using the estimates from table 4-1, the vector of mean values for the pH and log $PCO_2$ is

$$\boldsymbol{\mu} = \begin{pmatrix} \mu_{pH} \\ \mu_{PCO_2} \end{pmatrix} = \begin{pmatrix} \mathbf{7.83} \\ \mathbf{-2.50} \end{pmatrix} \tag{4-1}$$

and the vector of sample standard deviations for the pH and log $PCO_2$ is

$$\boldsymbol{\sigma} = \begin{pmatrix} \sigma_{pH} \\ \sigma_{PCO_2} \end{pmatrix} = \begin{pmatrix} \mathbf{0.45} \\ \mathbf{0.54} \end{pmatrix} \tag{4-2}$$

where bold symbols indicate vectors or matrices of appropriate dimension. Consider a column vector $\mathbf{v}$ consisting of a pair of independent standard normal deviates and a fixed transformation matrix $\mathbf{L}$ such that

$$\boldsymbol{\xi} = \mathbf{L}\mathbf{v} \tag{4-3}$$

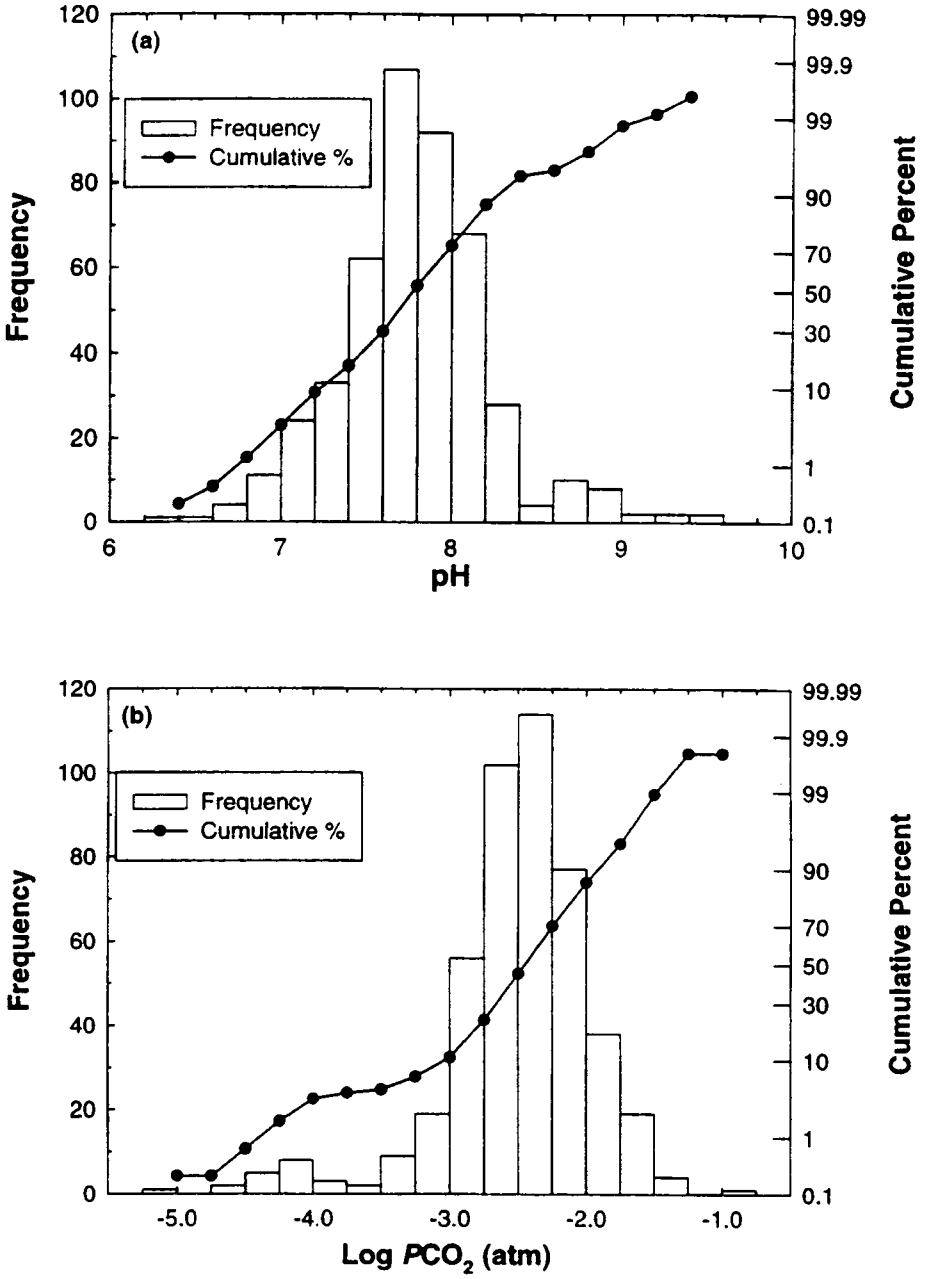


**Figure 4-1. Critical geochemical parameter values for 460 saturated zone regional groundwater samples collected in the vicinity of Yucca Mountain, Nevada [original data from Perfect et al. (1995); see Turner (1998) for screening criteria]. (a) pH and (b) log $PCO_2$ calculated using major ion chemical analyses and MINTEQA2, Version 3.11**

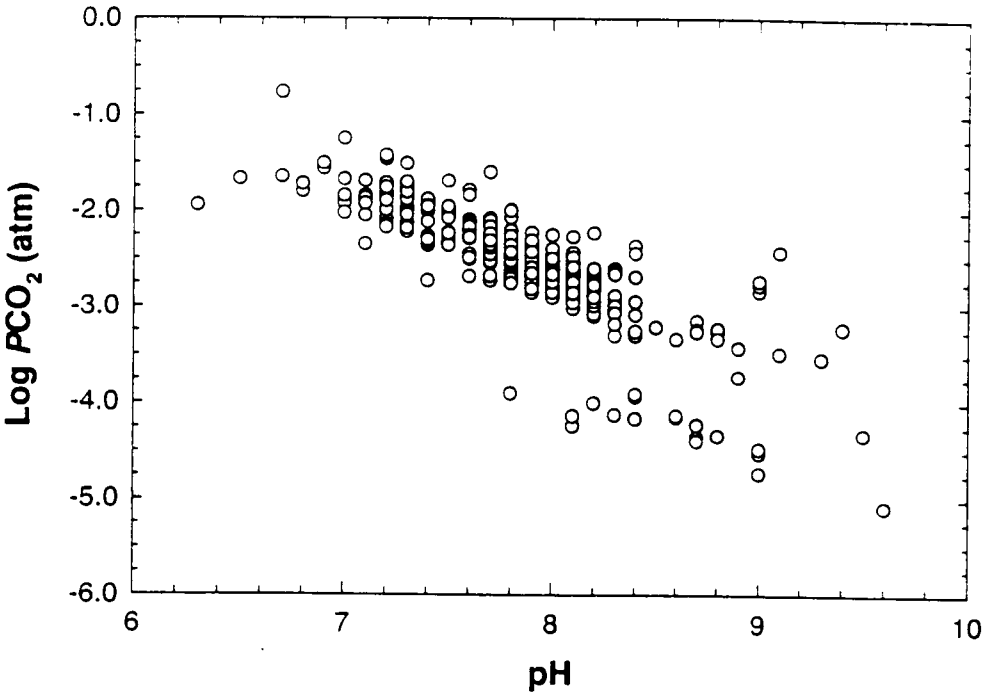


**Figure 4-2. Measured pH versus log $PCO_2$ for 460 saturated zone regional samples collected in the vicinity of Yucca Mountain, Nevada [original data from Perfect et al. (1995); see Turner (1998) for screening criteria]**

where $\xi$ is jointly normal with zero mean and covariance matrix $\Omega$. Using the correlation coefficient between pH and log $PCO_2$ and the standard deviations estimated from the raw data, the covariance matrix is

$$\Omega = \begin{pmatrix} \sigma^2_{pH} & \rho_{PCO_2,pH}\sigma_{pH}\sigma_{PCO_2} \\ \rho_{pH,PCO_2}\ \sigma_{PCO_2}\sigma_{pH} & \sigma^2_{PCO_2} \end{pmatrix} = \begin{pmatrix} 0.1985 & -0.2007 \\ -0.2007 & 0.2943 \end{pmatrix} \quad (4\text{-}4)$$

where the actual numbers will vary slightly depending on rounding. By definition

$$E(\xi\xi^T) = E(Lvv^TL^T) = LE(vv^T)L^T = \Omega \quad (4\text{-}5)$$

but

$$E(vv^T) = I \quad (4\text{-}6)$$

the identity matrix. Therefore

$$\mathbf{L}\mathbf{L}^{T} = \boldsymbol{\Omega} \tag{4-7}$$

where $\mathbf{L}$ is the lower triangle of the Cholesky decomposition (Atkinson, 1978) of the covariance matrix $\boldsymbol{\Omega}$. Once $\mathbf{L}$ is determined, jointly normal random values of the pH and log $PCO_2$ are constructed by first generating the vector of independent standard normal deviates, $\boldsymbol{\nu}$, and performing the transformation

$$\boldsymbol{\xi} = \mathbf{L}\boldsymbol{\nu} + \boldsymbol{\mu} \tag{4-8}$$

or

$$\begin{pmatrix} \xi_{pH} \\ \xi_{PCO_2} \end{pmatrix} = \begin{pmatrix} 0.45 & 0 \\ -0.4504 & 0.3024 \end{pmatrix} \begin{pmatrix} \nu_{pH} \\ \nu_{PCO_2} \end{pmatrix} + \begin{pmatrix} 7.83 \\ -2.50 \end{pmatrix} \tag{4-9}$$

The resulting values are plotted in figure 4-3. Comparison of figure 4-3 with figure 4-2 indicates that the sampled ranges for both pH and log $PCO_2$ are slightly narrower than the observed ambient groundwater chemistry, particularly at lower values of log $PCO_2$. This may be in part because of the assumption of a log-normal distribution of log $PCO_2$, when there are a small number ($\lesssim 12$) of low $PCO_2$ waters in the 460 measured groundwaters investigated by Turner (1998).

Sorption coefficients were estimated for Np(V) sorption on montmorillonite ($A' = 10\ m^2/g$) by interpolating the $K_D$ response surface defined by the polynomials presented in table 3-2 (figure 4-4). As might be expected given the narrower ranges in sampled pH and log $PCO_2$ relative to the measured values, the $K_D$ range estimated using the response surface is narrower than the range calculated directly from the measured water chemistries (Turner, 1998). A 3D representation of response surface-calculated $K_{A'}$ versus pH and $PCO_2$ (figure 4-5) shows a similar trend to that estimated in figure 2-7. The $K_D$s estimated using the response surface tend to be lower than those calculated directly by the DLM; and in this sense the use of a response surface in PA would be a conservative approach. Larger numbers of sampled pH and $PCO_2$ might provide more sampling of extreme conditions, but the assumption of a normal distribution may not take into account observed extremes.

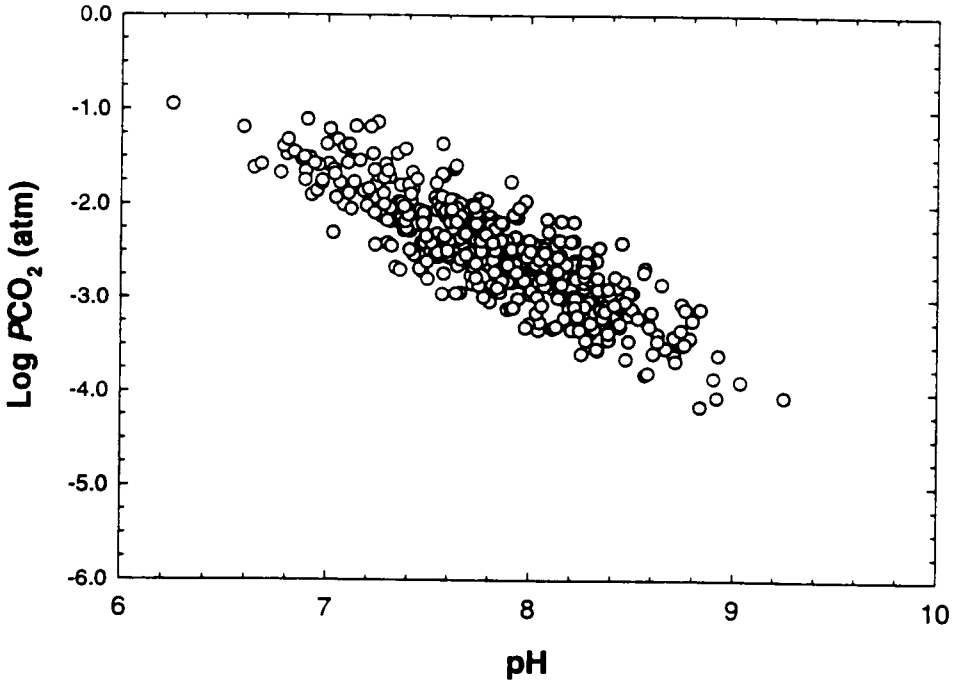


**Figure 4-3. Sampled pH versus log $PCO_2$ calculated using the population statistics provided in table 4-1 and shown in figures 4-1 and 4-2**

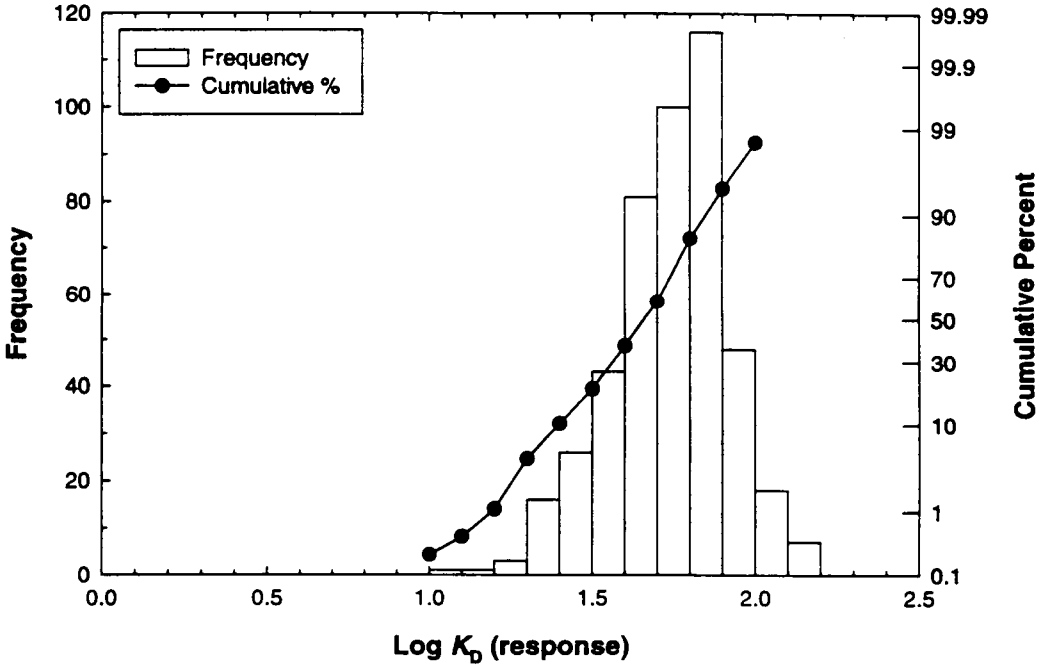


**Figure 4-4. Log $K_D$ calculated from the response surface defined by the polynomial equations given in table 3-2 and shown in figure 3-2.**

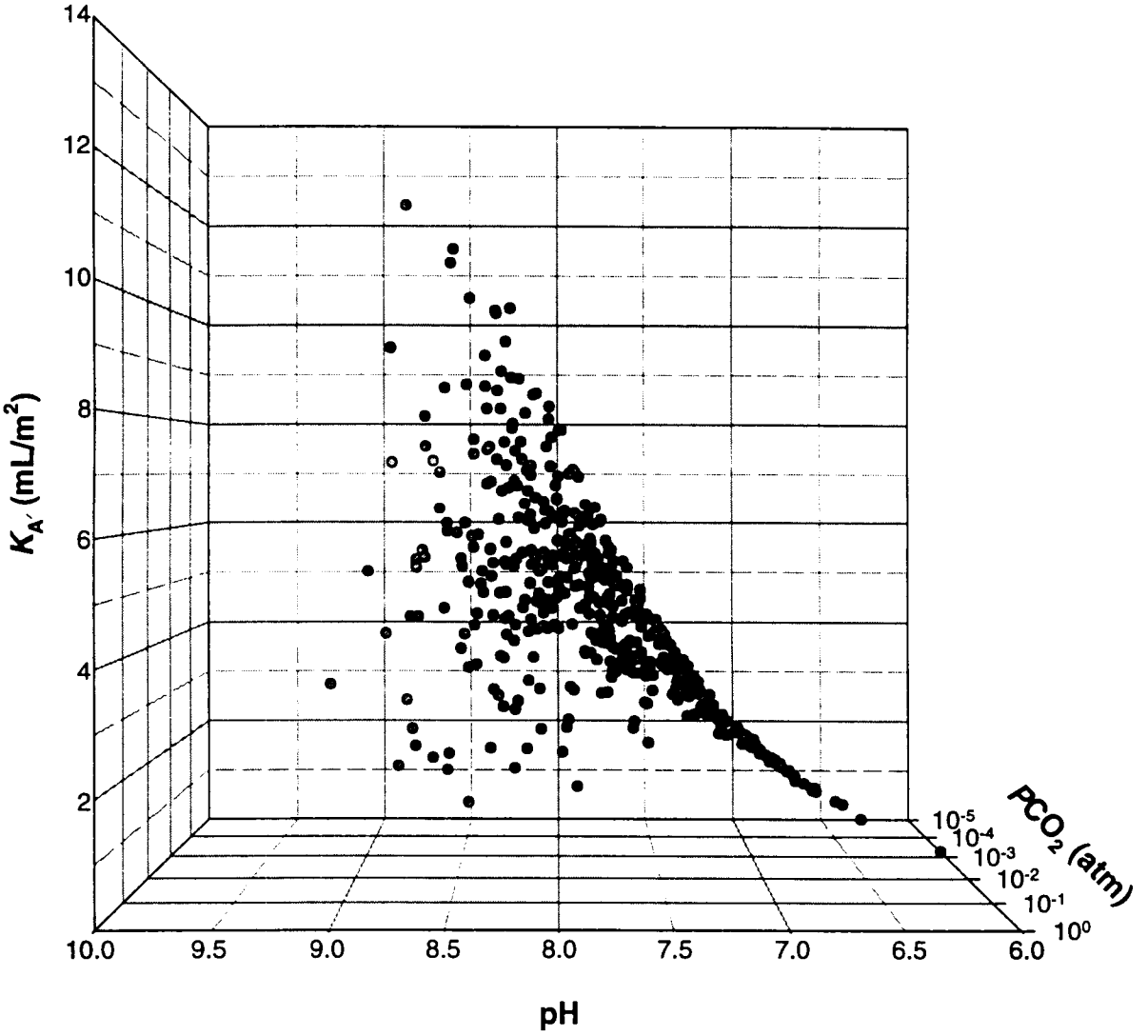


**Figure 4-5. Three-dimensional representation of $K_{A'}$ shown as a function of pH and $PCO_2$, calculated from the response surface defined by the polynomial equations given in table 3-2 and shown in figure 3-2.**

# 5 SUMMARY AND CONCLUSIONS

Identifying and evaluating processes affecting RT through alluvium was identified as a subissue in the RT KTI (Nuclear Regulatory Commission, 1998). Certain geochemical processes can both retard RT, delaying arrival times at the critical group location(s), and reduce radionuclide concentrations at the point of exposure. An understanding of geochemical processes that influence RT may be used to compensate for uncertainties in hydrologic models of the YM system (Simmons et al., 1995).

Ideally, mechanistic sorption models such as SCMs would be directly incorporated into reactive transport codes. While hydrogeochemical transport codes may be used to examine particular aspects of reactive transport, the additional computational burden that results from coupling equations for geochemistry and fluid flow may be excessive for PA. This is even more important for stochastic approaches that rely on sampling techniques and many realizations to generate complementary cumulative distribution functions and population statistics. It may be possible to use the DLM off-line to support $K_D$ selection and assess the effect of critical parameters such as pH and $PCO_2$ for site-specific conditions.

One means of using the DLM is to apply the model over a wide range of geochemical conditions and develop a sorption response surface as a function of key parameters. Unlike $K_D$, which is a derived value, geochemical parameters are properties of the physical-chemical system that can either be measured or assigned bounding limits. The calculated sorbed and aqueous concentrations can be used to develop a range in $K_D$ values predicted as a function of these variables. While this is not an explicit incorporation of geochemistry in the transport calculations, it does provide a step toward a more theoretical basis for sorption modeling in PA.

Based on the evaluation of options for incorporation of the sorption module into TPA, a sample flow chart (figure 5-1) is presented using the combination look-up table and mathematical representation of the response surface. Required data for the sorption module include solution pH, $PCO_2$ (or equivalent), and mineral surface area.

The SCM used here accurately reproduces experimental data over the range on which the model is based and appears to be applicable for more than one mineral type. Mineral surface or rock surface areas may be used since the model appears to have the potential for applicability to a number of minerals, especially silicates. Comparisons to data from similar mineral types conducted over a broader range of conditions show the model is applicable to a spectrum of Np(V) concentration or produces conservative estimates of sorption while maintaining the ability to represent changes in sorption behavior owing to modifications in system chemistry (e.g., pH and $PCO_2$). The insensitivity to M/V and Np(V) concentration within the model implies that a limited number of variables need be provided and suggests that generated $K_D$s may be independent of flowpath or changes in Np(V) concentration because of sorption. Only changes in $PCO_2$ and pH need be considered. It is important to note that the model presented here is for one radionuclide only. In practice, PA typically tracks many radionuclides, each of which will require its own set of SCM parameters, as well as unique response surface and descriptive equations.

Problems with the model include a lack of (i) consideration for ion exchange, (ii) confirmation/validation with experimental data collected over a range of conditions addressed by the model (such as M/V), and, (iii) data confirming applicability to multiple mineral types.

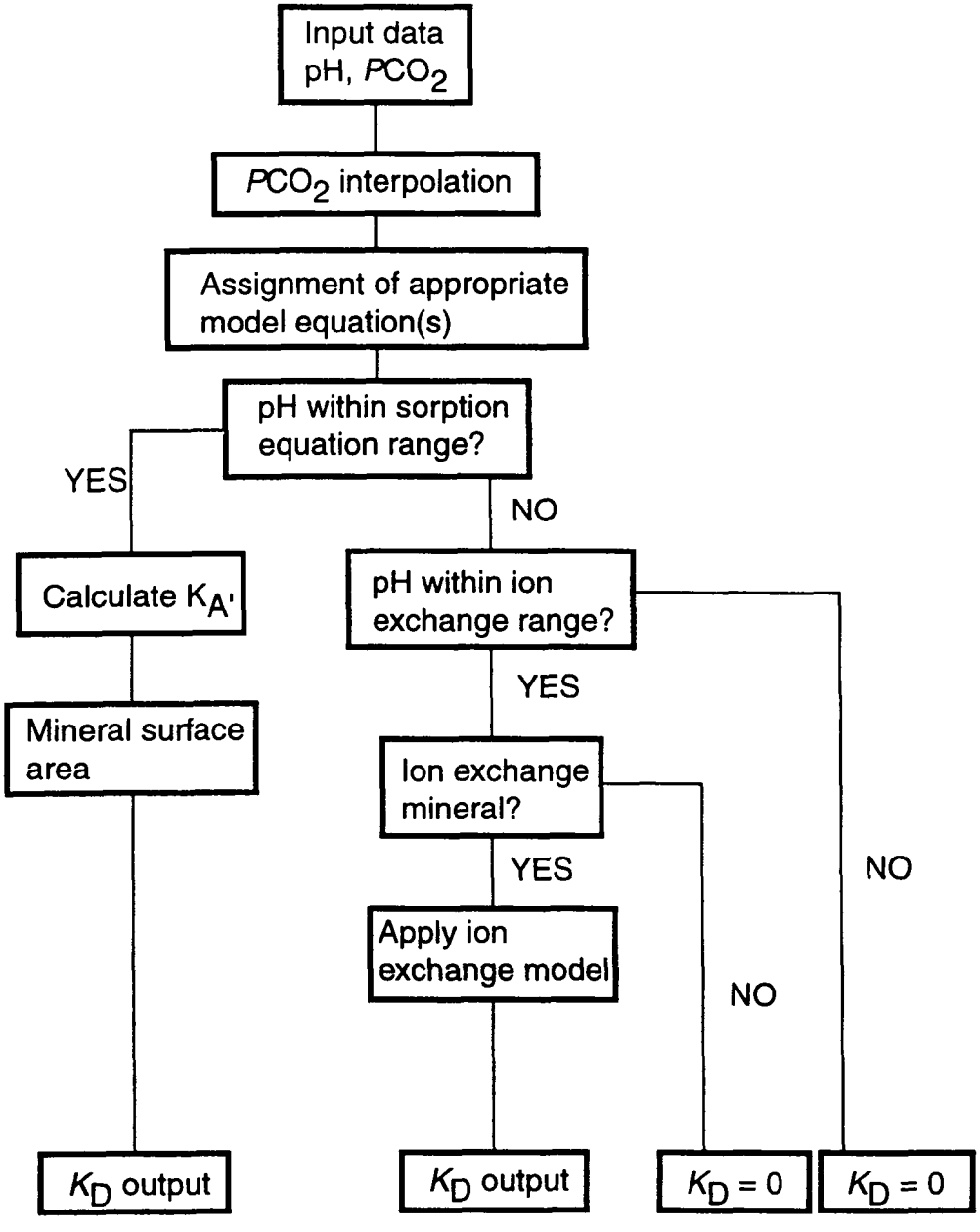


**Figure 5-1. Flow diagram showing an approach that can be used to incorporate geochemical sorption models in performance assessment**

Considerations for future work in the application of this approach to PA should include (i) assessment of a similar approach for other radionuclides, (ii) extension of modeling to incorporate more than one set of experiments for development of surface reactions and binding constants, (iii) evaluation of the utility of incorporating an ion exchange module, and (iv) development of experiments that would aid in the validation of the model.

# 6 REFERENCES


Allard, B., U. Olofsson, and B. Torstenfelt. 1984. Environmental actinide chemistry. *Inorganica Chimica Acta* 94: 205–221.

Allison, J.D., D.S. Brown, and K.J. Novo-Gradac. 1991. *MINTEQA2/PRODEFA2, a Geochemical Assessment Model for Environmental Systems: Version 3.0 User's Manual*, EPA/600/3-91/021. Athens, GA: Environmental Protection Agency.

Atkinson, K.E. 1978. *An Introduction to Numerical Analysis*. New York: John Wiley and Sons.

Beall, G.W., and B. Allard. 1981. Sorption of actinides from aqueous solutions under environmental conditions. *Adsorption from Aqueous Solutions*. P.H Tewari, ed. New York: Plenum Press.

Bertetti, F.P., R.T. Pabalan, D.R. Turner, and M.G. Almendarez. 1996. Neptunium(V) sorption behavior on clinoptilolite, quartz and montmorillonite. *Scientific Basis for Nuclear Waste Management XVII*. W.M. Murphy and D.A. Knecht, eds. Pittsburgh, PA: Materials Research Society: Symposium Proceedings 412: 631–638.

Bertetti, F.P., R.T. Pabalan, and M.G. Almendarez. 1998. Studies of neptunium$^{V}$ sorption on quartz, clinoptilolite, montmorillonite, and α-alumina. E.A. Jenne, ed. *Adsorption of Metals by Geomedia*. New York: Academic Press, Inc.

Claassen, H.C. 1985. *Sources and Mechanisms of Recharge for Ground Water in the West-Central Amargosa Desert, Nevada—A Geochemical Interpretation*. U.S. Geological Survey Professional Paper 712-F. Washington, DC: U.S. Geological Survey.

Cornwall, H.R. 1972. *Geology and Mineral Deposits of Southern Nye County, Nevada*. Nevada Bureau of Mines and Geology Bulletin 77. Reno, NV: Nevada Bureau of Mines and Geology.

Danesi P.R., R. Chiarizia, G. Scibona, and G.J. D'Alessandro. 1971. Stability constants of nitrate and chloride complexes of Np(IV), Np(V) and Np(VI) ions. *Inorganic Nuclear Chemistry* 33: 3,503–3,510.

Davis, J.A., and J.O. Leckie. 1978. Surface ionization and complexation at the oxide/water interface 2. Surface properties of amorphous iron oxyhydroxide and adsorption of metal ions. *Journal of Colloid and Interface Science* 67: 90–107.

Davis, J.A., and D.B. Kent. 1990. Surface complexation modeling in aqueous geochemistry. *Reviews in Mineralogy: Volume 23. Mineral-Water Interface Geochemistry*. M.F. Hochella, Jr. and A.F. White, eds. Washington, DC: Mineralogical Society of America: 177–260.

Dzombak, D.A., and F.M.M. Morel. 1990. *Surface Complexation Modeling: Hydrous Ferric Oxide*. New York: John Wiley and Sons.

Fuger, J. 1992. Thermodynamic properties of actinide species relevant to geochemical problems. *Radiochimica Acta* 59: 81–91.

Hayes, K.F., G. Redden, W. Ela, and J.O. Leckie. 1991. Surface complexation models: An evaluation of model parameter estimation using FITEQL and oxide mineral titration data. *Journal of Colloid and Interface Science* 142: 448–469.

Legoux, Y., G. Blain, R. Guillamont, G. Ouzounian, L. Brillard, and M. Hussonnois. 1992. $K_D$ measurements of activation, fission and heavy elements in water/solid phase systems. *Radiochimica Acta* 58/59: 211–218.

Lemire, R.J. 1984. *An Assessment of the Thermodynamic Behavior of Neptunium in Water and Model Groundwaters from 25 to 150 °C.* AECL–7817. Pinawa, Manitoba: Atomic Energy of Canada Limited.

Lemire R.J., and F. Garisto. 1989. *The Solubility of U, Np, Pu, Th, and Tc in a Geologic Disposal Vault for Used Nuclear Fuel.* AECL–10009. Pinawa, Manitoba: Atomic Energy of Canada Limited.

Lemire R.J., G.D. Boyer, and A.B. Campbell. 1993. The solubilities of sodium and potassium dioxoneptunium(V) carbonate hydrates at 30, 50 and 75°C. *Radiochimica Acta* 61: 57–63.

Meyer, R.E., W.D. Arnold, and F.I. Case. 1985. *Valence Effects on the Sorption of Nuclides on Rocks and Minerals II.* NUREG/CR–4114, ORNL–6137. Oak Ridge, TN: Oak Ridge National Laboratory.

Murphy, W.M., and R.T. Pabalan. 1994. *Geochemical Investigations Related to the Yucca Mountain Environment and Potential Nuclear Waste Repository.* NUREG/CR–6288. Washington, DC: Nuclear Regulatory Commission.

National Research Council. 1992. *Ground Water at Yucca Mountain: How High Can It Rise?.* Washington, DC: National Academy Press.

Nuclear Regulatory Commission. 1998. *Issue Resolution Status Report on Radionuclide Transport.* Washington, DC: Nuclear Regulatory Commission.

Pabalan, R.T., D.R. Turner, F.P. Bertetti, and J.D. Prikryl. 1998. Uranium$^{VI}$ sorption onto selected mineral surfaces. E.A. Jenne, ed. *Adsorption of Metals by Geomedia.* New York: Adademic Press, Inc.

Perfect, D.L., C.C. Faunt, W.C. Steinkampf, and A.K. Turner. 1995. *Hydrochemical Data Base for the Death Valley Region, California and Nevada.* USGS Open-File Report 94-305. Denver, CO: U.S. Geological Survey.

Righetto, L., G. Bidoglio, G. Azimonti, and I.R. Bellobono. 1991. Competitive actinide interactions in colloidal humic acid-mineral oxide systems. *Environmental Science and Technology* 25: 1,913–1,919.

Simmons, A.M., S.T. Nelson, P.L. Cloke, T.R. Crump, C.J. Duffy, W.E. Glassley, Z.E. Peterman, M.D. Siegel, D. Stahl, W.C. Steinkampf, and B.E. Viani. 1995. *The Critical Role of Geochemistry in the Program Approach.* Department of Energy Letter Report. Washington, DC: U.S. Department of Energy.

Torstenfelt, B., R.S. Rundberg, and A.J. Mitchell. 1988. Actinide sorption on granites and minerals as a function of colloids/pseudocolloids. *Radiochimica Acta* 44/45: 111–117.

TRW Environmental Safety Systems, Inc. 1995. *Total System Performance Assessment—1995: An Evaluation of the Potential Yucca Mountain Repository.* B00000000–01717–2200–00136. Las Vegas, NV: TRW Environmental Safety Systems, Inc.

Turner, D.R. 1995. *A Uniform Approach to Surface Complexation Modeling of Radionuclide Sorption.* CNWRA 95-001. San Antonio, TX: Center for Nuclear Waste Regulatory Analyses.

Turner, D.R. 1998. *Radionuclide Sorption in Fractures at Yucca Mountain, Nevada: A Preliminary Demonstration of Approach for Performance Assessment.* San Antonio, TX: Center for Nuclear Waste Regulatory Analyses.

Turner, D.R., and S.A. Sassman. 1996. Approaches to sorption modeling for high-level waste performance assessment. *Journal of Contaminant Hydrology* 21: 311–332.

Turner, D.R., R.T. Pabalan, and F.P. Bertetti. 1998. Neptunium(V) sorption on montmorillonite: An experimental and surface complexation modeling study. *Clays and Clay Minerals.* In press.

U.S. Department of Energy. 1996. Highlights of the U.S. Department of Energy's updated waste containment and isolation strategy for the yucca mountain site. Denver, CO. DOE concurrence draft. *Presentation to the Nuclear Waste Technical Review Board.* July 1996.

U.S. Department of Energy. 1998. *Repository Safety Strategy: U.S. Department of Energy's Strategy to Protect Public Health and Safety After Closure of a Yucca Mountain Repository.* Revision 1. Washington, DC: U.S. Department of Energy, Office of Civilian Radioactive Waste Management.

Wescott, R.G., M.P. Lee, N.A. Eisenberg, and T.J. McCartin. 1995. *NRC Iterative Performance Assessment Phase 2: Development of Capabilities for Review of a Performance Assessment for a High-Level Waste Repository.* NUREG–1464. Washington, DC: Nuclear Regulatory Commission.

Westall, J.C., and H. Hohl. 1980. A comparison of electrostatic models for the oxide/solution interface. *Advances in Colloid and Interface Science* 12: 265–294.

Wilson, M.L., J.H. Gauthier, R.W. Barnard, G.E. Barr, and H.A. Dockery, E. Dunn, R.R. Eaton, D.C. Guerin, N. Lu, M.J. Martinez, R. Nilson, C.A. Rautman, T.H. Robey, B. Ross, E.E. Ryder, A.R. Schenker, S.A. Shannon, L.H. Skinner, W.G. Halsey, J.D. Gansemer, L.C. Lewis, A.D. Lamont, I.R. Triay, A. Meijer, and D.E. Morris. 1994. *Total-System Performance Assessment for Yucca Mountain—SNL Second Iteration (TSPA-1993).* Volume 2. SAND93–2675. Albuquerque, NM: Sandia National Laboratories.